BBA Clinical 5 (2016) 1–15

Contents lists available at ScienceDirect

BBA Clinical

journal homepage: www.elsevier.com/locate/bbaclin

Glioblastomas with copy number gains in *EGFR* and *RNF139* show increased expressions of carbonic anhydrase genes transformed by *ENO1*

Marie E. Beckner [a,*,2], Ian F. Pollack [b,c], Mary L. Nordberg [d,e], Ronald L. Hamilton [f]

[a] Department of Neurology, Louisiana State University Health Sciences Center-Shreveport, RM. 3-438, 1501 Kings Highway, Shreveport, LA 71130, United States [1]
[b] Department of Neurological Surgery, University of Pittsburgh School of Medicine, United States
[c] 4th Floor, Children's Hospital of Pittsburgh, UPMC, 4129 Penn Avenue, Pittsburgh, PA 15224, United States
[d] Department of Medicine, Louisiana State University Health, 1501 Kings Highway, Shreveport, LA 71130, United States
[e] The Delta Pathology Group, One Saint Mary Place, Shreveport, LA 71101, United States
[f] Department of Pathology, Division of Neuropathology, S724.1, Scaife Hall, University of Pittsburgh School of Medicine, 3550 Terrace Street, Pittsburgh, PA 15261, United States

ARTICLE INFO

Article history:
Received 12 August 2015
Received in revised form 17 October 2015
Accepted 2 November 2015
Available online 10 November 2015

Keywords:
Amplified oncogenes
Glycolysis
Carbonic anhydrase
EGFR
RNF139
XIAP

ABSTRACT

Background: Prominence of glycolysis in glioblastomas may be non-specific or a feature of oncogene-related subgroups (i.e. amplified *EGFR*, etc.). Relationships between amplified oncogenes and expressions of metabolic genes associated with glycolysis, directly or indirectly via pH, were therefore investigated.
Methods: Using multiplex ligation-dependent probe amplification, copy numbers (CN) of 78 oncogenes were quantified in 24 glioblastomas. Related expressions of metabolic genes encoding lactate dehydrogenases (*LDHA*, *LDHC*), carbonic anhydrases (*CA3*, *CA12*), monocarboxylate transporters (*SLC16A3* or *MCT4*, *SLC16A4* or *MCT5*), ATP citrate lyase (*ACLY*), glycogen synthase1 (*GYS1*), hypoxia inducible factor-1A (*HIF1A*), and enolase1 (*ENO1*) were determined in 22 by RT-qPCR. To obtain supra-glycolytic levels and adjust for heterogeneity, concurrent *ENO1* expression was used to mathematically transform the expression levels of metabolic genes already normalized with delta-delta crossing threshold methodology.
Results: Positive correlations with *EGFR* occurred for all metabolic genes. Significant differences (Wilcoxon Rank Sum) for oncogene CN gains in tumors of at least 2.00-fold versus less than 2.00-fold occurred for *EGFR* with *CA3*'s expression ($p < 0.03$) and for *RNF139* with *CA12* ($p < 0.004$). Increased CN of *XIAP* associated negatively. Tumors with less than 2.00-fold CN gains differed from those with gains for *XIAP* with *CA12* ($p < 0.05$). Male gender associated with *CA12* ($p < 0.05$).
Conclusions: Glioblastomas with CN increases in *EGFR* had elevated *CA3* expression. Similarly, tumors with *RNF149* CN gains had elevated *CA12* expression.
General significance: In larger studies, subgroups of glioblastomas may emerge according to oncogene-related effects on glycolysis, such as control of pH via effects on carbonic anhydrases, with prognostic and treatment implications.

1. Introduction

Increased reliance on glycolysis for ATP is a defining feature of malignancies, including the incurable, high-grade brain tumors known as glioblastomas. Enzymes of the glycolytic pathway in tumors are protected under conditions that are inhospitable for normal cells. In previous studies of glioblastoma cells, we identified their pseudopodia as being glycolytic subcellular domains that also contain oncogene products, including increased Met [1] and phosphorylated *EGFR*. Discovering increased anti-phosphotyrosine and anti-phosphoserine/threonine-reactive bands on immunoblots of pseudopodia compared to whole cells suggested to us that multiple oncogenes could be present in glycolytic regions of these cells (unpublished). In view of the functional roles and associations of the proteins encoded by oncogenes in enhancement of tumors and their malignant behavior, oncogenes

Abbreviations: CN, copy number; DAPI, diaminephylindole; ddCt, delta-delta crossing threshold; GB, glioblastoma; GOI, gene of interest; HKG, housekeeping gene; IRES, internal ribosome entry site; MLPA, multiplex ligation-dependent probe amplification; MPNST, malignant peripheral nerve sheath tumor; MTB/GF, metabolic/growth factor; NB, normal brain; RT-qPCR, real time quantitative PCR; REMBRANDT, Repository of Molecular Brain Neoplasia Database; SLC, solute carrier; WHO, World Health Organization.

* Corresponding author at: School of Biomedical Sciences, Kent State University, Kent, OH, United States.
E-mail addresses: mbeckne1@kent.edu, mbeckner@sprynet.com (M.E. Beckner), pollaci@upmc.edu, ian.pollack@chp.edu (I.F. Pollack), mary.nordberg@deltamdx.com (M.L. Nordberg).
[1] (former position)
[2] present address: School of Biomedical Sciences, Kent State University, 256 Cunningham Hall, P.O. Box 5190, Kent, OH 44242-0001, United States.

http://dx.doi.org/10.1016/j.bbacli.2015.11.001

that are amplified are logical candidates to investigate for aiding glycolysis. Oncogenes and their products potentially increase protection of glycolytic enzymes from the protons released by non-aerobic production of ATP involving lactic acid.

Copy numbers (CNs) of amplified oncogenes and expression levels of metabolic genes can be determined in the same tumors to detect functional associations. PCR techniques quantify gene expression and CN with impressive sensitivity. Heterogeneity within each tumor due to a malformed vasculature, etc. leads to fluctuation in metabolism. To account for heterogeneity in levels of glycolytic activity and obtain supra-glycolytic levels, the expression results for metabolic genes in tumor samples were transformed mathematically to levels indicated by expression of *ENO1* that encodes enolase 1, the major isoform of enolase in glioblastomas. Enolase catalyzes the ninth of ten steps in the traditional glycolytic pathway. The expression of *ENO1* in tumors, given as a value relative to normal brain expression, was used to scale the expression levels of other metabolic genes in the same tumor. The metabolic genes' expression levels were transformed to be multiples of concurrent *ENO1* levels. Studies have shown that *ENO1* is seldom lost in high grade brain tumors. *ENO1* was retained in 98.6% of glioblastomas with some variation in expression levels noted [2]. Expressing each metabolic gene as a multiple of *ENO1*'s expression level in the same sample led to the discovery of positive correlations between oncogene CNs and the expression of metabolic genes in this study. Possibly glioblastomas harbor functional subgroups defined by changes in CN of oncogenes.

Not surprisingly, including control of pH among the functional choices of genes to study yielded significant results. Warburg utilized large amounts of bicarbonate in his model of cancer [3]. The bicarbonate buffer system is the most important physiologic buffer. It controls the body's pH via independent regulation of its components, carbon dioxide and bicarbonate, by the lungs and kidneys, respectively, thus providing tremendous capacity [4]. Determining how tumors take advantage of the circulating 4300 mmoles of bicarbonate that the kidneys filter and mostly recycle daily [5] is urgently needed. Our study identified multiple associations between *EGFR*, *RNF139*, and *XIAP* oncogenes and gender with expression levels of two carbonic anhydrases that catalyze interconversions among components of the bicarbonate buffer system.

2. Materials and methods

2.1. Patients in the study

With patient and Institutional Review Board approval, frozen samples of glioblastomas resected from 25 adult patients during the time interval, 2002–2008, were obtained from the University of Pittsburgh Brain Tumor Tissue Bank. Clinical information for 24 patients included a mean age of 62.9 yr., range 19–81 yr., M:F = 11:13, and data for specific patients are listed (Table 1). Only one case, GB25, was unsatisfactory for all parts of the study.

Table 1
Clinical information regarding glioblastoma (GB) patients.

GB	Age (yrs)	Sex	GB	Age (yrs)	Sex
01	36	M	13	66	M
02	57	M	14	53	M
03	77	F	15	69	F
04	58	F	16	19	M
05	43	F	17	78	F
06	59	F	18	65	M
07	74	F	19	62	F
08	69	F	20	69	F
09	Unk[a]	Unk	21	80	M
10	46	M	22	81	F
11	69	M	23	55	F
12	64	M	24	80	M
			25	81	F

[a] Unknown data.

2.2. Multiplex ligation-dependent probe amplification (MLPA) analysis of oncogenes

Copy number (CN) was determined for each of seventy-eight oncogenes (*AKT1*, *AURKA*, *BCAR3*, *BCAS1* and *2*, *BCL2*, *BCL2A1*, *BCL2L1*, *11*, *13*, *and 14*, *BCL6*, *BCLG*, *BIRC2*, *3*, and *5*, *BRAF*, *BRMS1*, *CCNA1*, *CCND1* and *2*, *CCNE1*, *CDK4* and *6*, *CENPF*, *CTTN*, *CYP27B1*, *EGFR*, *ERBB2* and *4*, *ESR1*, *EVI1*, *FGF3* and *4*, *FGFR1*, *GNAS*, *GSTP1*, *HMGA1*, *IGF1R*, *IGFBP2*, *4* and *5*, *IRS2*, *JAK2*, *MDM2* and *4*, *MET*, *MMP7*, *MOS*, *MYCL*, *MYBL1* and *2*, *MYC*, *MYCN*, *NAIP*, *NFKBIE*, *NRAS*, *NTRK1-3*, *PDGFRA* and *B*, *PIK3C2B*, *PIK3CA*, *PPM1D*, *PSMB4*, *PTK2*, *PTP4A3*, *PTPN1*, *RELA*, *RNF139*, *RUNX1*, *SERBINB2*, *7*, and *9*, *TERT*, *TOM1L2*, *UCKL1*, *and XIAP*). Multiplex ligation-dependent probe amplification (MLPA) was successfully performed in 24 tumors (GB01-GB24) to obtain CN data. Normal brain (NB) from the occipital lobe of an 82 yr. old female (Biochain, Hayward, CA) was used to normalize tumor DNA results for each oncogene's CN. All tumors were analyzed concurrently with NB in the MLPA assays. Briefly, in MLPA, DNA (200 ng) from tumor samples and NB was denatured at 98 °C and hybridized with MLPA probes (P171, P172, P173 Tumor Gains kits, MRC-Holland, The Netherlands) for genes that are known to be amplified in tumors. Hybridization occurred during 16–20 h at 60 °C. Ligations with Ligase65 (MRC-Holland) were at 54 °C for 15 min followed by 98 °C for 5 min. Ligation products were amplified with PCR primers and polymerase for 35 cycles (30 s 95 °C, 30 s 60 °C, 60 s 72 °C) and then 20 min at 72 °C at the end using a thermocycler (MasterCycler personal Eppendorf, Hamburg, GM). PCR products were separated and analyzed via capillary electrophoresis using the SS600 Fragment Analysis option with fluorescent signal detection on a CEQ8000 instrument (Beckman-Coulter, Fullerton, CA) using the manufacturer's reagents and size standards. Stuffer sequences incorporated into PCR probes of specific lengths identified the amplified products of PCR reactions in regard to each gene. Peak heights reflected initial amounts of DNA. Slightly less efficient PCR of longer amplicons accounted for minor reductions in peak heights that were corrected with NB by dividing tumor oncogene CN by NB CN for the same oncogene. These methods have been previously described more fully [6,7]. Note that in earlier studies *BCL2L14* was listed as *BCLG/BCL2L14*, *CTTN* as *EMS*, *NAIP* as *BIRC1*, *XIAP* as *BIRC4*, and *UCKL1* as *FLJ20517*. Some cytogenetic loci for various genes have also changed and are given in this paper as they are currently listed on the Online Mendelian Inheritance in Man (OMIM) or HUGO Gene Nomenclature Committee (HGNC) websites, http://www.omim.org/ and http://www.genenames.org/, respectively.

2.3. RT-qPCR for metabolic and growth factor (MTB/GF) gene expression

Numerous genes encoding proteins that favor glycolysis under adverse conditions, including acidosis and intermittent disconnection from the blood supply (i.e. invasive cell migration), were considered among genes whose encoded proteins enable glycolysis during hypoxia. Using early (2007–2008) versions of the Repository of Molecular Brain Neoplasia Database (REMBRANDT) [8], *ENO1* was chosen to represent the expression levels of genes encoding enzymes in the energy generation phase of glycolysis and then served to transform expressions of other metabolic genes and growth factor genes. Nine other genes (*ACLY*, *CA3*, *CA12*, *GYS1*, *HIF1A*, *LDHA*, *LDHC*, *SLC16A3* (or *MCT4*), and *SLC16A4*) were chosen as genes of interest (GOI) from the functionally relevant metabolic groups of genes. Two growth factors, *EGF* and *PDGFA*, were also chosen for this study. For each group of genes (glucose transport, glycolysis, mitochondria, links between metabolic pathways, fat metabolism, control of pH/lactate, glycogen metabolism, gluconeogenesis, and growth factors) and for each individual gene, the prevalence of 2-fold or greater elevations in glioblastomas, the likelihood

of a glioma being a glioblastoma if an elevation in expression was present, significantly poorer survival in glioblastomas with elevations (see Section 3.2), as well as functional relevance based on previous studies, were considered in compiling a list of 12 metabolic/growth factor (MTB/GF) genes to study for associations with oncogenes. Data for the MTB/GF genes in their respective groups and the controls are given in Section 3.2. Since *ENO1* was used for MTB/GF gene transformations and *SLC16A4*'s locus was potentially within an oncogene amplicon (see Section 3.1), data is reported most comprehensively for eight of the ten metabolic genes. The RNA-derived cDNAs were prepared from tumor samples and the reference pooled non-malignant brain RNA from 23 adults, mean 68.3 yr., range 23–86 yr. of age. Sufficient RNA was obtained from 22 tumors (GB01-08 and GB10-23) for analysis (M:F = 10:12, 19–80 yr. of age). Template cDNAs in each tumor and the reference were tested in triplicate for quantitative expression levels of MTB/GF genes and two housekeeping genes (HKGs), which were *ACTB* and *GAPDH* on 96 well plates (SABioSciences Corp. Qiagen, Valencia, CA), using an ABI 7500 Prism thermocycler (Applied BioSystems, ThermoFisher Scientific, Waltham, MA). The delta-delta crossing threshold (ddCt) method was used to determine fold increases in the tumors compared to reference derived cDNA with averaged HKGs used for normalization. Each dCt equaled Ct(MTB/GF)—average Ct(HKG). The ddCt for each gene equaled dCt(tumor sample) — dCt(reference non-malignant brain). The fold-change for each MTB/GF gene compared to the normal reference was equal to 2^{-ddCt}. This methodology and the HKGs have been more fully described [9]. After normalizing with the HKGs, MTB/GF gene expression levels were transformed (division by concurrent expression of *ENO1*). Results for each MTB/GF gene were used for comparisons with CN of oncogenes in Fisher's Exact tests, correlations, and Wilcoxon Rank Sum comparisons.

2.4. Detection of MTB gene relationships with the presence of any amplified oncogenes

Tumors were initially stratified according to whether they had oncogene(s) amplified at 3.00-fold or greater levels (Yes or No) to facilitate analysis with Fisher Exact tests. The results for each MTB/GF gene were used to determine tumor membership in Group (+) if the MTB/GF gene had ≥1.10× (times) *ENO1* expression and Group (−) if the MTB/GF gene had <1.10× *ENO1* expression levels. The cut-off of 1.10× expression of *ENO1* was chosen to form the groups with no other cut-offs attempted to avoid selection bias. The 1.10× threshold was used only for the Fisher Exact tests reported in Section 3.4.

2.5. EGFR fluorescence in situ hybridization (FISH)

A frozen tissue sample available on GB06 was evaluated for *EGFR* signals with fluorescence in situ hybridization (FISH). The FISH probes for the *EGFR* band region, 7p11.2–7p12 and a control locus, 7p11.1–q11.1, D7Z1, (Vysis Locus Specific Identifier *EGFR* SpectrumOrange and CEP 7 SpectrumGreen, respectively, Abbott Molecular Inc., Des Plaines, IL) were hybridized to interphase nuclei in a 5 μm section overnight. Un-hybridized probes were washed away. Diaminophylindole (DAPI) fluorescent blue (Abbott Molecular) stained the nuclei. Slides were scanned on a fluorescent microscope (Leica DMR, Wetzlar, GM) for analysis with images captured using a digital camera (Applied Imaging, San Jose, CA) and CytoVision v4.02 imaging software (Applied Imaging). The methodology was described in a previous study [6].

2.6. Statistical tests

The Fisher's Exact tests were described in Section 2.4. Pearson's correlation coefficients were calculated to detect positive and negative correlations between expression values of MTB/GF genes and CN of oncogenes. Correlations were also performed for 3 genes in the 8q amplicon with each other. Wilcoxon Rank Sum comparisons were performed to detect associations with metabolic gene expression in the group of oncogenes defined by (1) exhibiting at least one 3.00-fold CN gain among all the tumors and (2) whose data yielded two groups of comparable sizes (10 and 12, 9 and 13, or 8 and 14 tumors) when oncogene CN gains of 2.00-fold or greater were considered. Associations with metabolic gene expressions have *p*-values stated for trends and significance levels less than 0.05. Also, chi square analyses were performed on tumors in the REMBRANDT database during the selection of genes for expression analysis, as described in the Results section (end of Section 3.2).

3. Results

3.1. Oncogene amplifications detected with MLPA

Twenty-four glioblastomas (GB1–GB24) assayed with MLPA for the CN levels of 78 oncogenes yielded amplifications, 3.00-fold or greater, in 18 glioblastomas for one or more of twenty oncogenes, listed as follows: *BCL2A1*, *CCND1*, *CCND2*, *CDK4*, *CDK6*, *CTTN*, *CYP27B1*, *EGFR*, *EVI1*, *FGF3*, *FGF4*, *GNAS*, *MDM4*, *MOS*, *MYC*, *PDGFRA*, *PIK3C2B*, *PIK3CA*, *RNF139*, and *XIAP*. Low level gains in CN that did not achieve a 3.00-fold threshold also occurred frequently. For the twenty oncogenes with at least one 3.00-fold amplification in the tumors, all of the CN gains for each one that were 2.00-fold or greater are shown at their chromosomal loci (Fig. 1). Locations of MTB/GF genes for which only RNA expression data were determined in the study are also included. Each of the 24 glioblastomas tested had at least one of the CN gains shown. Genes not amplified at or beyond the 3.00-fold threshold in at least one tumor are not shown. Tumors with CN gains of *EGFR* also had CN gains of one to seven other oncogenes among those shown (Fig. 1). Twelve genes, whose gains were always below 3.00-fold among the glioblastomas, included *NRAS* (1p13.2), *BCAS2* (1p13.2), *ERBB4* (2q34), *BCL6* (3q27.3), *NAIP* (5q13.2), *MET* (7q31.2), *BRAF* (7q34), *MDM2* (12q15), *PPM1D* (17q23.2), *BCL2L1* (20q11.21), *AURKA* (20q13.2), and *RUNX1* (21q22.12), in at least one of 23 tumors. Of these, *MDM2* was co-amplified along with *CYP27B1 and CDK4* nearby on chromosome 12 in GB19, and with only *CYP27B1* in GB14. These findings are consistent with the complexity of the 12q13-15 amplicon described in glioblastomas [10]. Also, *AURKA* was co-amplified with nearby *GNAS* on chromosome 20 in GB06.

It was noted that near or at the locus for *SLC16A4* (1p13.3), CN gains occurred for oncogenes, *NRAS* (1p13.2) and *BCAS2* (1p13.3). Although results for *SLC16A4* are included when those for all the MTB/GF genes are listed in tables, they are not shown when results of metabolic genes are highlighted as a group (eight genes remaining) in the following figures due to the possibility that *SLC16A4* was a bystander in an amplicon containing the oncogenes, *NRAS* and *BCAS2*. Also, deletions of oncogenes detected are not reported in this study. An example of MLPA amplification results for *PDGFRA* and *EGFR* are shown for GB06 with FISH signals for *EGFR* in the frozen sample included as an insert (Fig. 2).

3.2. Expression of metabolic/growth factor (MTB/GF) genes in REMBRANDT

Specific members of functional groups and gene families were chosen for study of their expression levels in samples of glioblastomas based on queries of the REMBRANDT database of brain tumors [8] and their potential support of glycolysis (Fig. 3a).

The highest proportions of 2-fold increased gene expressions occurred among the following functional groups: the energy generation phase of glycolysis, anaerobic glycolysis, upregulation of glycolysis, links between metabolic pathways, control of pH/lactate, glycogen metabolism, and growth factors. Within four of these groups, *ENO1*, *LDHC*, *CA3*, and *ACLY* had the greatest numbers of elevations for expression.

Additionally, in regard to the anaerobic glycolysis group, elevations of *LDHA* expression levels at least 2-fold were present in 14 of all the

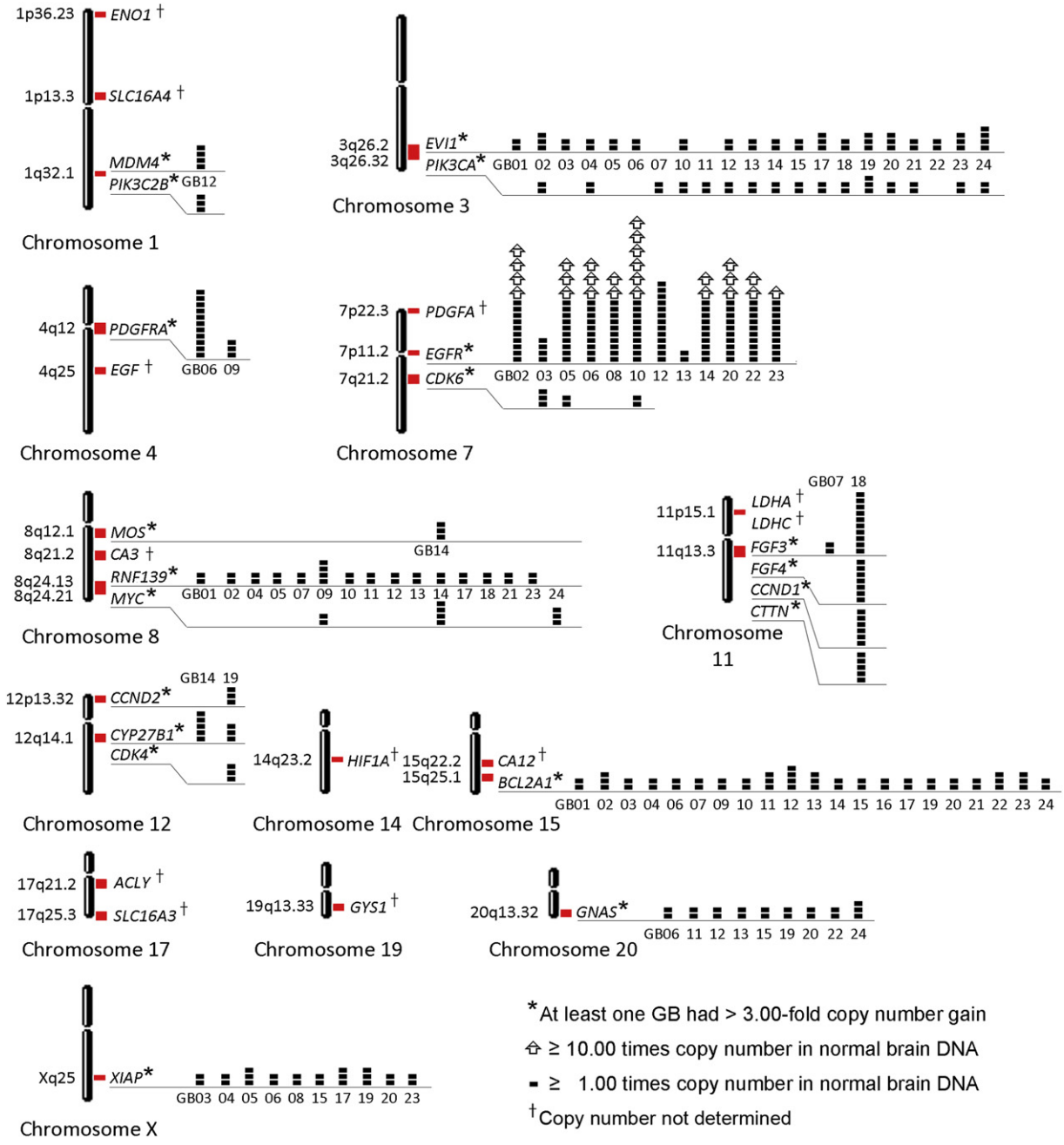

Fig. 1. Loci of amplified oncogenes and metabolic/growth factor genes. The chromosomal loci (red rectangles) of twenty oncogenes amplified at least 3.00-fold and metabolic/growth factor (MTB/GF) genes are shown. The copy number (CN) amplification of oncogenes in each glioblastoma (GB) are depicted with small solid black rectangles (1.00 times normal per rectangle) and open arrows (10.00 times normal per arrow) as indicated in comparison to normal brain DNA. The highest CN gains occurred for *EGFR*. The superscript (†) indicates the MTB/GF genes with expression data but no CN data.

gliomas so that if it was elevated in a glioma, there was a 92.9% chance that the tumor was a glioblastoma. The chances of a glioma with 2-fold or greater elevations of *LDHC* or *ENO1* for being a glioblastoma were 85.7% and 89.3%, respectively. Therefore *LDHA* was also included. Results for *CA12* and *SCL16A4* (Fig. 3b) were comparable to *CA3*'s results, along with impressive significantly poorer survival results at high expression levels, therefore they were also included. The well-known function of the protein encoded by *SLC16A3* (better known as MCT4) and occurrence of its results within the range of the other chosen members in this functional group warranted its inclusion.

Within the glycogen metabolism group, *GYS1*, *GBE*, and *PYGL* had at least 2-fold elevations in 36, 101, and 114 gliomas, respectively, with poorer Kaplan Meier survival in all gliomas for each of the three genes at such significant levels that their *p*-values were all given as 0.0. The chances of the elevations occurring in a glioblastoma, when present in a glioma, were 88.9%, 73.3%, and 70.2%, respectively, for *GYS1*, *GBE1*, and *PYGL*. With this data, along with functional data reported previously [11], *GYS1* was chosen to study. Elevations of at least 2-fold expression among the growth factors, *EGF*, *PDGFA*, *TGFB1*, and *TGFB2* occurred in 32, 52, 58, and 66, respectively, of all gliomas so the tumors with elevations were also glioblastomas at rates of 75.0%, 76.9%, 70.7%, and 74.2%, respectively. Considering this data along with the abundance of literature supporting their roles in brain tumors, *EGF* and *PDGFA*, were chosen. Also, later searches showed that increased expression of *EGF* was present in a higher percentage of glioblastomas than the 2007 REMBRANDT data indicated. The well-known regulator of glycolysis in hypoxia, *HIF1A*, was also included. Functions of the proteins encoded by the MTB/GF and control genes are given (Table 2).

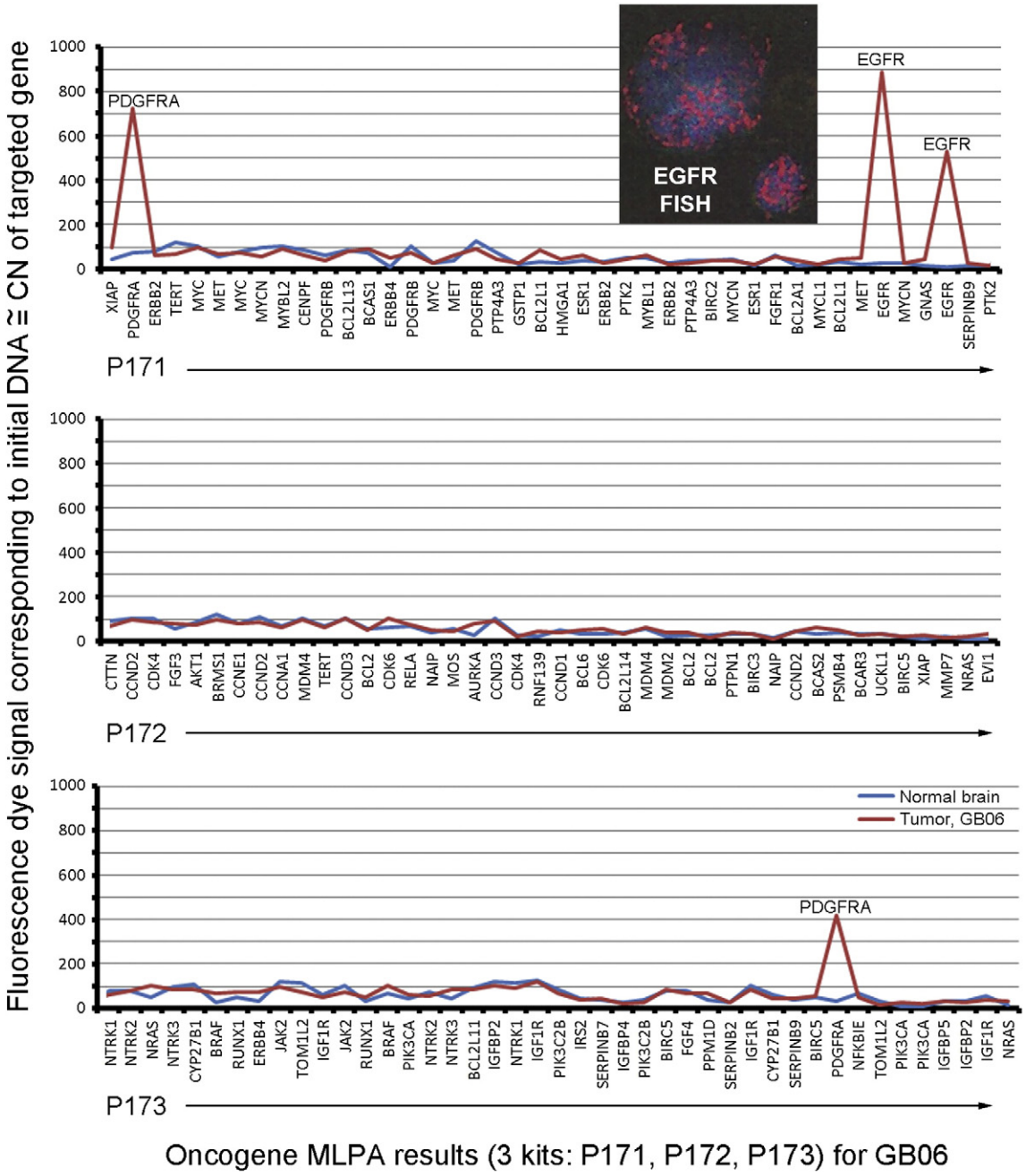

Fig. 2. Quantified oncogenes in GB06. An example of multiplex ligation-dependent probe amplification (MLPA) results for 78 oncogenes in one glioblastoma. Its high level amplifications of *PDGFRA* and *EGFR* were readily detected as fluorescence signals from each of the 2 sets of probes used for each oncogene. The two-fold elevations in tumor versus normal brain were detected using mathematical comparisons described in Section 2.2. The red and blue lines represent tumor and normal DNA, respectively. Also, the inset at the top shows fluorescence in situ hybridization (FISH) signals for *EGFR* (red) in two cells of the frozen tissue sample used for MLPA. The nuclei stained blue with diaminophylindole (DAPI).

In support of these choices, significantly poorer Kaplan Meier survival in all gliomas was reported in the database for *ACLY*, *GYS1*, *ENO1*, and *HIF1A*, at 2 or 3-fold levels of increased gene expression. The other chosen metabolic genes, *CA3*, *CA12*, *SLC16A3* (or *MCT4*), *SCL16A4*, *LDHA*, and *LDHC*, had significantly poorer survival in glioblastomas with increased expression at levels that varied from 2 to 10-fold above normal. Also, *EGF* and *PDGFA* had significantly poorer survival associated with elevated expression levels in all gliomas and glioblastomas and in all gliomas, respectively. Additionally, by chi square analyses the likelihood for elevated levels of the genes to occur in a glioblastoma that also contained a 2-fold elevation in expression of *ENO1* (our putative indicator of glycolytic activity) was $p < 0.05$ for *ACLY*, *GYS1*, *SLC16A4*, *LDHA*, and *HIF1A*. Trends for *PDGFA*, *LDHC*, *SLC16A3* (or *MCT4*), and *EGF* occurred with *p*-values of 0.05, 0.05, 0.14, and 0.16, respectively. Specific *p*-values for the expression of *CA3* at 3-fold, 7-fold, and 10-fold elevations to occur in tumors with 2-fold elevations in *ENO1's* expression were 0.48, 0.27, and 0.25, respectively. The downward trend in *p*-values for fold elevations of *CA3* extending to the highest limit in the database was valued. The *p*-values for expression of *CA12* at 2-fold, 3-fold, and 5-fold elevations to occur in tumors with 2-fold elevations in *ENO1*'s expression were 0.04, 0.002, and 0.0001, respectively.

3.3. MTB/GF gene expression mathematically transformed by concurrent *ENO1* levels

RNA from 22 glioblastomas in this study yielded results that could be analyzed with RT-qPCR. One of the unsatisfactory specimens (GB25)

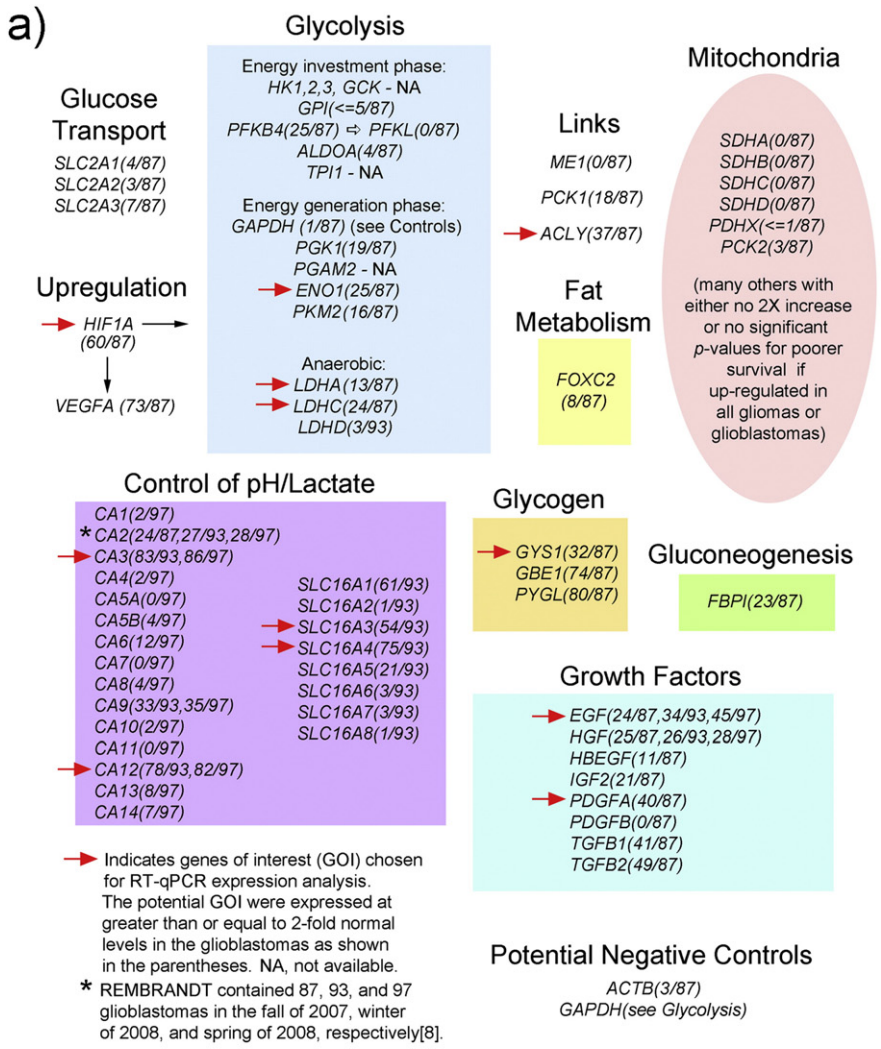

b)

Expression Levels ↑	CA2	CA3	CA9	CA12	SLC16A1	SLC16A3	SCL16A4
2-fold	(24/87)(27/93)(28/97)	(83/93)(86/97)	(33/93)(35/97)	(78/93)(82/97)	(61/93)	(54/93)	**(75/93)**
3-fold	(3/97)	(64/93)(67/97)	(20/93)(21/97)	(65/93)(69/97)	(32/93)	(34/93)	**(63/93)**
4-fold		**(57/93)(59/97)**	(13/93)(14/97)	(50/93)(54/97)	(12/93)	**(17/93)**	**(50/93)**
5-fold		(52/93)(54/97)	(9/93)(10/97)	(39/93)**(42/97)**	(6/93)	(14/93)	**(42/93)**
6-fold		(45/93)(47/97)	(5/97)	**(30/93)(32/97)**		(11/93)	**(36/93)**
7-fold		**(40/93)(42/97)**		**(27/93)(28/97)**		(10/93)	**(32/93)**
8-fold		**(37/93)(39/97)**		**(17/93)**(18/97)			**(25/93)**
9-fold		**(35/93)**(37/97)		**(15/93)(16/97)**			**(20/93)**
10-fold		**(33/93)(35/97)**		**(14/93)(15/97)**			**(18/93)**

Fig. 3. Searches for MTB/GF genes of interest (GOI) in the REMBRANDT database. Genes were chosen based on functional relevance and REMBRANDT [8] expression data. Section 3.2 explains the selection of GOI indicated with red arrows in detail. (a) Functional groupings. (b) Utilization of expression levels above two-fold in selection of GOI in the carbonic anhydrase and solute carrier 16 families of genes. Expression levels that had significant *p*-values (<0.05) for poorer survival (Kaplan Meier) are bolded. The full gene names are as follows: *ACLY* (*ATP citrate lyase*), *ACTB* (*actin B*), *ALDOA* (*aldolase A*), *CA* (*carbonic anhydrase*), *EGF* (*epidermal growth factor*), *ENO1* (*enolase 1*), *FBP1* (*fructose 1,6 bisphosphatase*), *FOXC2* (*forkhead box C2*), *GAPDH* (*glyceraldehyde-3-phosphate dehydrogenase*), *GBE1* (*glycogen binding enzyme*), *GCK* (*glucokinase*), *GPI* (*glucophosphoisomerase*), *GYS1* (*glycogen synthase 1*), *HBEGF* (*heparin-binding EGF like growth factor*), *HGF* (*hepatocyte growth factor*), *HIF1A* (*hypoxia-inducible factor 1, alpha subunit*), *HK* (*hexokinase*), *IGF2* (*insulin-like growth factor II*), *LDH* (*lactate dehydrogenase*), *ME1* (*malic enzyme 1*), *PCK* (*phosphoenolpyruvate carboxykinase*), *PDGF* (*platelet-derived growth factor*), *PDHX* (*pyruvate dehydrogenase complex, component X*), *PFKFB4* (*6-phosphofructo-2-kinase/fructose-2,6 bisphosphatase 4*), *PGAM2* (*phosphoglycerate mutase 2*), *PGK1* (*phosphoglycerate kinase 1*), *PFKL* (*phosphofructokinase L*), *PKM2* (*pyruvate kinase, muscle, 2*), *PYGL* (*glycogen phosphorylase, liver*), *SDH* (*succinate dehydrogenase complex*), *SLC2* (*solute carrier family 2*), *SLC16* (*solute carrier family 16*), *TGFB* (*transforming growth factor, beta*), and *TPI1* (*triosephosphate isomerase 1*). Note that *SCL16A3* is also known as *MCT4* (*monocarboxylate transporter 4*).

was also unsatisfactory for MLPA when determining CN of oncogenes. The concurrent values for expression of *ENO1*, ranging from 0.222 to 1.972 times normal, were used to transform the expression of each MTB/GF gene to multiples of *ENO1* to reflect their levels relative to glycolytic pathway activity to obtain the supra-glycolytic levels in adjusting for tumor heterogeneity. The range of gene expression for pathway activity was assumed to range from 0.222 to 1.972 times normal according to the values of *ENO1*. In a previous study the expression

Table 2
Functions of proteins encoded by metabolic and growth factor (MTB/GF) genes selected for expression analysis and studies for associations with oncogenes.

1. *ACLY*, *ATP citrate lyase*	Cleaves citric acid, synthesizes acetyl CoA
2. *CA3*, *Carbonic anhydrase III*	Interconversions of CO_2/HCO_3^- in cytoplasm
3. *CA12*, *Carbonic anhydrase XII*	Interconversions of CO_2/HCO_3^- at cell surface
4. *ENO1*, *Enolase 1*[*]	Catalyzes ninth of ten steps in glycolysis
5. *GYS1*, *Glycogen synthase 1*	Synthesis of glycogen from simpler carbohydrates
6. *HIF1A*, *Hypoxia-inducible factor 1, alpha subunit*	Transcription factor, upregulates genes in hypoxia
7. *LDHA*, *Lactate Dehydrogenase A*	Interconversion of lactic acid and pyruvate
8. *LDHC*, *Lactate Dehydrogenase C*[ǂ]	Interconversion of lactic acid and pyruvate
9. *SLC16A3, Solute carrier family 16 (monocarboxylic acid transporter), member 3.* See protein name	Transports lactic acid and pyruvate across membranes, protein called monocarboxylate transporter 4 (MCT4)
10. *SLC16A4, Solute carrier family 16 (monocarboxylic acid transporter), member 4.* See protein name	Transports lactic acid and pyruvate across membranes, proteincalled monocarboxylate transporter 5 (MCT5)
11. *EGF*, *Epidermal Growth Factor*	Differentiation, etc.
12. *PDGFA*,*Platelet-derived growth factor, alpha polypeptide*	Mesenchymal cell mitogenesis, etc.
13. *ACTB*, *Actin B*	Structural, Housekeeping gene (HKG) for RT-qPCR
14. *GAPDH*, *Glyceraldehyde-3-phosphate dehydrogenase*	Glycolysis, Housekeeping gene (HKG) for RT-qPCR

[*] *ENO1* was used to transform the expression levels of the other MTB/GF genes.
[ǂ] *LDHC* gene expression was originally thought to be limited to testes but has been found in various types of malignancy.

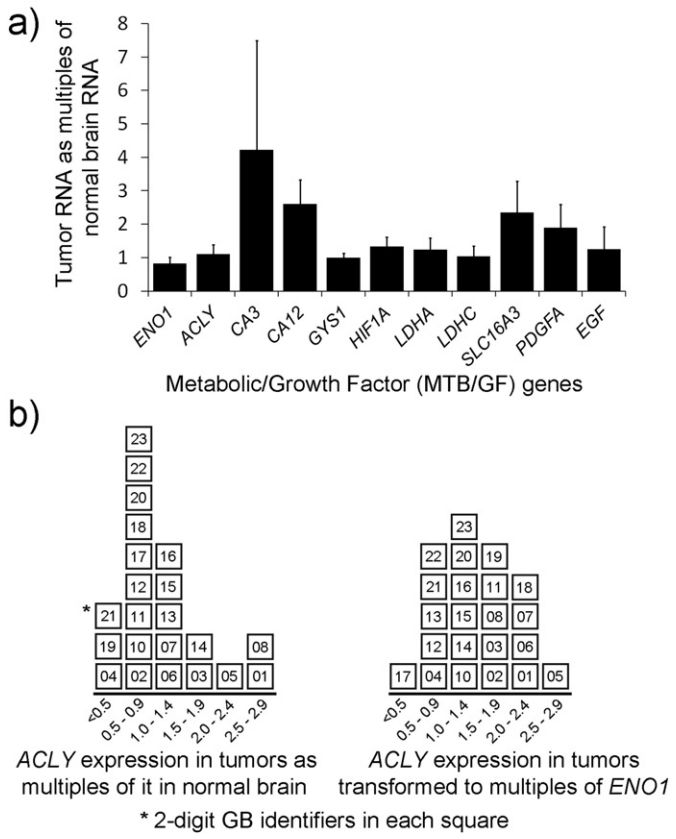

Fig. 4. Expressions of MTB/GF genes and the effect of *ENO1* transformation on *ACLY* in considering *ENO1* as a candidate for MTB/GF transformations. (a) Comparisons of MTB/GF gene expressions, including *ENO1*, prior to transformations in 22 glioblastomas (GBs). Normal brain RNA was from pooled non-malignant brain tissue. Each gene's fold change was obtained with the ddCt method described in Section 2.3. Means with 95% confidence intervals are shown for each gene. (b) Effects of *ENO1* when used to transform a metabolic gene's expression data. On the left, the distribution of GBs, each identified with a 2-digit number, is displayed according to *ACLY*'s expression in each as a fold-change compared to normal brain's *ACLY* RNA. The distribution shown on the right is according to each tumor's expression of *ACLY* following transformation (division by concurrent *ENO1* expression).

of *ACLY* in this group of tumors was shown to correlate with concurrent expression of *ENO1* with no transformation performed and minus one outlier [9]. The mean expressions of MTB/GF genes with 95% confidence intervals (CI) are shown for all 22 glioblastomas (Fig. 4a).

The medians were within the lower halves of the 95% CI shown, except for *GYS1* and *SLC16A3* (or *MCT4*). *GYS1*'s median was in the upper half of the 95% CI shown. *SLC16A3*'s median was not in the gene's 95% CI and its 1st, 2nd (median), and 3rd quartiles were 0.668, 1.378, and 3.340, respectively. *CA3* with the largest degree of variability shown had 1st, 2nd, and 3rd quartiles of 0.822, 1.019, and 2.568, respectively. The distributions of 22 individual glioblastomas according to their expression of *ACLY*, before and after transformation with concurrent *ENO1*, are shown (Fig. 4b). The transformation produced results in the same range with GBs more evenly distributed. However, only 5 tumors retained the same level of expression and 7 shifted more than 1 level of expression that is indicated on the *x*-axis. Distributions of the glioblastomas according to their expressions of eight metabolic genes, after transformation with concurrent *ENO1* expressions can be compared to *ACLY*'s distribution (Fig. 5).

3.4. Fisher's exact tests of MTB/GF gene expression with oncogene copy number gains

Expression levels of the MTB/GF genes were transformed so that levels above those attributed to ongoing glycolysis in a heterogeneous tumor environment could be analyzed. After transforming their levels to represent multiples of *ENO1*'s concurrent expression, Groups (+) and (−) were obtained for each MTB/GF gene based on whether its expression level was equal to or greater than 1.10 times the expression of *ENO1* or not, respectively. Statistical significance, $p = 0.041$ (Fisher's Exact), for a difference was found for *LDHC*'s Group (+) as shown (Table 3, bottom row).

A tumor with elevated *LDHC* levels had a greater likelihood of having any 3.00-fold amplified oncogenes compared to Group(−) that was comprised of tumors with *LDHC* levels below the cut-off. In Group(+) for *LDHC*, 92% (11/12) of the tumors had amplified oncogenes versus 50% (5/10) in Group(−). The amplified oncogenes included *EGFR*, *EVI1*, *BCL2A1*, and *PIK3CA* in 8, 7, 6, and 3 tumors, respectively, with *EGFR* frequently being co-amplified. A strong tendency, $p = 0.085$ (Fisher's Exact), was also seen for the higher expression levels of *LDHA* to have amplified oncogenes, with 86% of its Group(+) having them versus 50% of its Group(−) tumors. Having only two glioblastomas in *CA12*'s Group(−) defined by this threshold limited its analysis.

3.5. Correlations of CN gains for oncogenes with expression of MTB/GF genes

Each of the twenty oncogenes with at least one 3.00-fold elevation among the glioblastomas exhibited positive correlations of their CN gains with increased expression levels of at least two MTB/GF genes (Table 4). All MTB/GF genes had positive correlations with CN of *EGFR* and also for sums of CN for all 20 oncogenes (not shown). Among the oncogenes, *CCND1* had the next highest frequency of positive correlations with MTB/GF genes and *PIK3C2B*, *PIK3CA*, *MOS*, *RNF139*, *CYP27B1*, and *BCL2A1*, each correlated positively with seven MTB/GF genes.

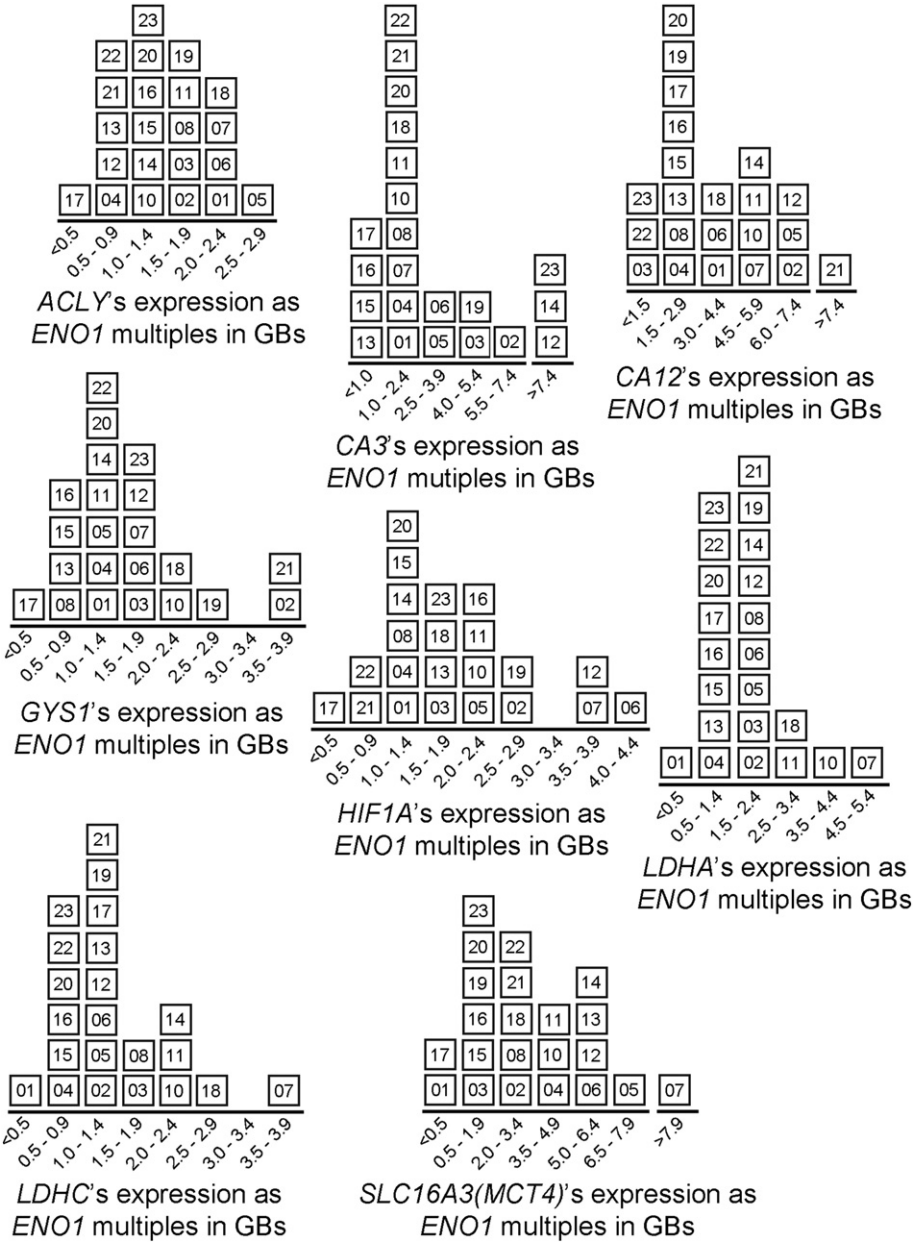

Fig. 5. Distributions of glioblastomas according their expressions of each metabolic gene following mathematical transformation by *ENO1*. This was described for *ACLY* (Fig. 4b). Each tumor is identified by a 2-digit number. The highest transformed values occurred for *CA3*, *CA12*, and *SCL16A3* (or *MCT4*).

In contrast, *XIAP* exhibited predominantly negative correlations and correlated positively with only two MTB/GF genes. Among the MTB/GF genes, *LCHC*, *LDHA*, and *GYS1* each had expression levels that correlated positively with CN of fourteen oncogenes that are listed. All of the metabolic genes had at least nine positive oncogene correlations each whereas the growth factor genes each had five. The highest individual correlation of a MTB/GF gene's expression with CN of an oncogene, $r = 0.63$, occurred for *PDGFA* with CN of *PDGFRA*, the gene for one of its receptors. The correlation of *HIF1A*'s expression with CN of *PDGFRA*, $r = 0.52$, was the next highest. The correlations of *CA3*'s expression with CN of *MOS* and *MYC*, $r = 0.46$ for each, were noted with the realization that all 3 genes are located on 8q (Fig. 1). Patterns for positive correlations in potential amplicons derived from 1q, 8q, 11q, and 12q occurred (Table 4, bottom row).

Also, two patterns of possible functional relevance emerged between metabolic genes and oncogenes. In one pattern, *LDHA*, *LDHC*, *CA3*, *CA12*, and *SLC16A3* (or *MCT4*), encoding proteins responsible for generation of ATP in anaerobic glycolysis and buffering of the resulting hydrogen ions, shared positive correlations with *MOS*, *RNF139*, *MYC*, *PIK3C2B*, *CYP27B1*, and *CDK4* as well as with *EGFR* (Table 4 and Fig. 6a). In a search for oncogenes that associate with glycolytic tumor cell migration [12], a second oncogene pattern was characterized by positive correlations of the lactate dehydrogenases and putative metabolic adaptors, *ACLY* and *GYS1* [9,11], for short-term or intermittent dependence on glycolysis. This group consisted of *ACLY*, *GYS1*, *LDHA*, and *LDHC*, positively correlating with the oncogenes, *CCND1*, *CTTN*, *FGF3*, *FGF4*, and *CCND2*, as well as with *EGFR*, (Table 4 and Fig. 6b). Strong negative correlations for five of the seven metabolic genes in these two groups were found for CN of *XIAP* (Table 4 and Fig. 6c).

3.6. Associations of metabolic gene expressions with CN of oncogenes and gender

Associations with CN of several oncogenes and gender were searched for among eight metabolic genes, *ACLY*, *CA3*, *CA12*, *GYS1*, *HIF1A*, *LDHA*, *LDHC*, and *SLC16A3* using Wilcoxon Rank Sum comparisons. There

Table 3
Stratification of each glioblastoma(GB) by the presence of amplified oncogenes and by expression levels of transformed metabolic/growth factor (MTB/GF) genes listed in the top row. Each MTB/GF level was divided by concurrent expression of *ENO1* to become a multiple of *ENO1* expression. If the result was ≥1.10 (arbitrary threshold), then the GB is included in Group (+) and otherwise is in Group (−). A significant (*$p < 0.05$) association for *LDHC* with the presence of amplified oncogenes and a trend for *LDHA* were detected in the GBs.

GB	Amplified oncogenes	*LDHC*	*LDHA*	*CA3*	*ACLY*	*GYS1*	*SLC16A3* (*MCT4*)	*SLC16A4* (*MCT5*)	*HIF1A*	*PDGFA*	*EGF*	*CA12*
01	No	−	−	−	+	+	−	+	+	−	−	+
02	Yes	+	+	+	+	+	+	+	+	+	+	+
03	Yes	+	+	+	+	+	−	−	+	+	+	−
04	No	−	−	+	−	−	+	−	−	+	+	+
05	Yes	+	+	+	+	+	+	+	+	+	+	+
06	Yes	+	+	+	+	+	+	+	+	+	+	+
07	No	+	+	+	+	+	+	+	+	+	+	+
08	Yes	+	+	+	+	−	+	−	−	+	−	+
10	Yes	+	+	+	+	+	+	+	+	+	−	+
11	Yes	+	+	+	+	+	+	+	+	+	−	+
12	Yes	+	+	+	−	+	+	+	+	−	−	+
13	Yes	−	+	−	−	−	+	−	+	−	−	+
14	Yes	+	+	+	+	−	+	+	+	−	+	+
15	No	−	−	−	−	−	−	−	+	+	+	+
16	No	−	−	−	+	−	−	−	+	−	−	+
17	Yes	−	−	−	−	−	−	+	−	−	−	+
18	Yes	+	+	+	+	+	+	+	+	+	+	+
19	Yes	+	+	+	+	+	+	−	+	−	−	+
20	Yes	−	−	−	+	+	−	−	+	+	−	+
21	No	−	+	+	−	+	+	+	−	+	−	+
22	Yes	−	−	−	−	+	+	+	−	−	−	−
23	Yes	−	−	+	+	+	−	+	+	+	+	+
Total in Group (−)		10	8	7	7	7	7	8	5	8	12	2
Total in Group (+)		12	14	15	15	15	15	14	17	14	10	20
Numerators = Number of GBs with at least one amplified oncogene (3-fold or greater) in Group(−) or Group(+)												
Group (−)		5/10	4/8	4/7	4/7	4/7	4/7	5/8	3/5	6/8	9/12	2/2
Group (+)		11/12	12/14	12/15	12/15	12/15	12/15	11/14	13/17	10/14	7/10	14/20
Fisher's Exact (p)		0.041*	0.085	0.213	0.213	0.213	0.213	0.273	0.319	0.376	0.354	0.519

were 4 oncogenes, *EGFR*, *RNF139*, *GNAS*, and *XIAP*, whose CN gains were sufficient in number among the glioblastomas (Fig. 1) so that comparisons could be made using 2.00-fold CN gains as the threshold for inclusion into one of two comparable-size groups for each of these four oncogenes. Additionally, stratification by gender (Table 1) also yielded comparable size groups. Due to *XIAP*'s location on the X chromosome, gender is a contributing factor to *XIAP*'s CN [13]. The gender ratio for those without *XIAP* CN gains of at least 2.00-fold was M:F = 10:2 and only females had *XIAP* CN gains that were 2.00-fold or more when standardized by normal DNA from a female for the CN studies. The largest number of significant associations occurred for *CA12*. Its associations with *RNF139*'s CN gains, *XIAP*'s lack of CN gains, and male gender, had p-values of 0.0037, 0.0426, and 0.0169, respectively, (Fig. 7a). Medians for *RNF139*'s CN gains, *XIAP*'s lack of gains, and male gender, all 5.1424 (level of *CA12* given as a multiple of concurrent *ENO1*'s expression) are shown as red dashed lines. The medians for *CA12*'s transformed expression levels in the opposing groups were 1.6024, 1.7213, and 1.7213, respectively, and are shown by blue dashed lines. A significant association occurred for *CA3* with 2.00-fold or greater CN gains of *EGFR*, $p = 0.0249$, with medians of 2.7444 and 1.2811 for *CA3*'s transformed expression levels in groups, with and without at least 2.00-fold CN gains of *EGFR*, respectively, (Fig. 7b). Strong trends for associations were found for transformed *LDHA*'s expression levels with *RNF139*'s 2.00-fold or greater CN gains, lack of *XIAP*'s CN gains, and male gender with p-values of 0.0950, 0.0804, and 0.1229, respectively, and a trend was also detected for an association between transformed *SLC16A3*(or *MCT4*)'s expression levels and *RNF139*'s 2.00-fold or greater CN gains, with a p-value of 0.11 (not shown). No significant associations or trends were found for *GNAS* using the 2.00-fold threshold for its CN gains with metabolic genes (not shown).

4. Discussion

When respiration is inhibited, such as during hypoxia, the glycolytic pathway lacks NAD^+ from mitochondria. To compensate, large amounts of the organic acid, lactate, are produced from pyruvate via lactate dehydrogenases to maintain the NAD^+ levels needed for continuous cycling of non-aerobic glycolysis. The capacity for buffering hydrogen ions becomes critical in glycolytic conditions due to susceptibility of phosphofructokinase and other glycolytic enzymes to inhibition by acidity [14–17], in addition to the sensitivity of many cellular proteins to pH changes. To control pH, there are alterations in carbonic anhydrase family members, solute carrier (SLC) family members that transport monocarboxylates, vacuolar type H^+-ATPases, membrane sodium/hydrogen exchangers, chloride/bicarbonate and sodium/bicarbonate exchangers, etc. that occur in a cooperative manner. Some of the regulation is known, such as the effect of HIF-1α on carbonic anhydrase IX and other proteins, but the complete picture is not known. The heightened activity of tumor cells to manipulate their pH for compensatory purposes is a hallmark of malignancy. This malignant feature has been implicated in drug resistance and provides new treatment targets to consider clinically [18–25].

The carbonic anhydrase family members are prominent mediators of pH control in tumors. The amounts of bicarbonate, HCO_3^-, needed to buffer protons would be depleted without replenishment by carbonic anhydrases that catalyze interconversions of carbon dioxide and water to bicarbonate and protons and vice versa via carbonic acid. The carbonic anhydrases possess impressively rapid catalytic rates, up to a million-fold maximal turnover rate per second for the carbonic anhydrase II isoform in red cells [26]. The catalytic rate of CAIII (encoded by *CA3*) in nucleated cells is slower but its activity can be enhanced by phosphates [27]. Also, isozyme-specific residues in the active site of CAIII, when replaced by their counterparts in CAII, permit CAIII to achieve the impressive kinetics of CAII [26,28,29]. Carbonic anhydrase III is a major protein in muscle and myoepithelial cells [30–32]. Expression of *CA3* and other genes, including *HIF1A*, were significantly augmented in muscle of endurance runners exercising in hypoxia (14.5% oxygen) [33]. In a separate study, repeated sprints by runners in hypoxia also led to increased expression levels of *CA3* [34]. Levels of CAIII also increase with age in human muscle [35]. In the central nervous system,

Table 4
Correlations between individual MTB/GF genes and copy numbers (CN) of oncogenes, listed horizontally, in 22 glioblastomas. Expression values of MTB/GF genes after ddCt normalization were divided by concurrent expression levels of normalized *ENO1* to obtain MTB/GF values as multiples of *ENO1*'s expression prior to calculating correlations. Positive correlations less than 0.2 are indicated by '+' and the negative ones are indicated by '-'. Genes are listed in the order of their chromosomal loci. Similar patterns of correlations for potential amplicons comprised of oncogenes are indicated in the bottom row. Note that *SLC16A3* is also known as *MCT4*.

MTB/GF genes listed below	1q32.1		3q26.2	3q26.32	4q12	7p11.2	7q21.2	8q12.1	8q24.13	8q24.21	11q13.3				12p13.32	12q14.1		15q25.1	20q13.32	Xq25
	MDM4	*PIK3C2B*	*EVI1*	*PIK3CA*	*PDGFRA*	*EGFR*	*CDK6*	*MOS*	*RNF139*	*MYC*	*CCND1*	*CTTN*	*FGF3*	*FGF4*	*CCND2*	*CYP27B1*	*CDK4*	*BCL2A1*	*GNAS*	*XIAP*
1p13.3																				
SLC16A4	−	−	−	+	0.28	+	−	+	+	−	+	−	−	−	−	−	−	0.24	0.22	+
4q25																				
EGF	−	−	+	−	0.39	0.25	0.37	−	−	−	−	−	−	−	−	−	−	−	−	+
7p22.3																				
PDGFA	−	−	−	−	0.63	0.40	+	−	−	−	−	−	−	−	−	−	−	+	0.27	−
8q21.2																				
CA3	0.33	0.34	0.24	+	−	+	+	0.46	0.35	0.46	−	−	−	−	−	0.41	0.44	0.36	+	0.00
11p15.1																				
LDHA	−	+	−	0.28	−	+	+	+	+	+	0.28	+	0.21	+	+	+	+	−	−	−
LDHC	−	+	−	0.27	−	+	+	0.26	+	+	0.42	0.31	0.37	0.30	+	+	+	−	−	−
14q23.2																				
HIF1A	0.34	0.46	−	+	0.52	+	−	−	−	−	+	−	−	−	0.21	−	−	0.34	0.38	−
15q22.2																				
CA12	0.31	0.33	+	+	−	+	−	+	0.39	+	+	−	−	−	−	+	+	0.19	−	−
17q21.2																				
ACLY	−	−	−	−	0.31	+	+	+	−	−	0.36	0.33	0.34	0.30	+	+	−	−	−	−
17q25.3																				
SLC16A3	+	0.21	−	−	0.20	+	−	0.27	0.20	0.23	+	−	−	−	−	+	+	+	+	−
19q13.33																				
GYS1	+	+	0.30	0.33	+	0.21	−	−	+	−	+	+	+	+	0.26	+	−	+	−	−
Similar patterns for the potential amplicons	9 of 11 MTB/GF genes							8 of 11 MTB/GF genes			7 of 11 MTB/GF genes					9 of 11 MTB/GF genes				

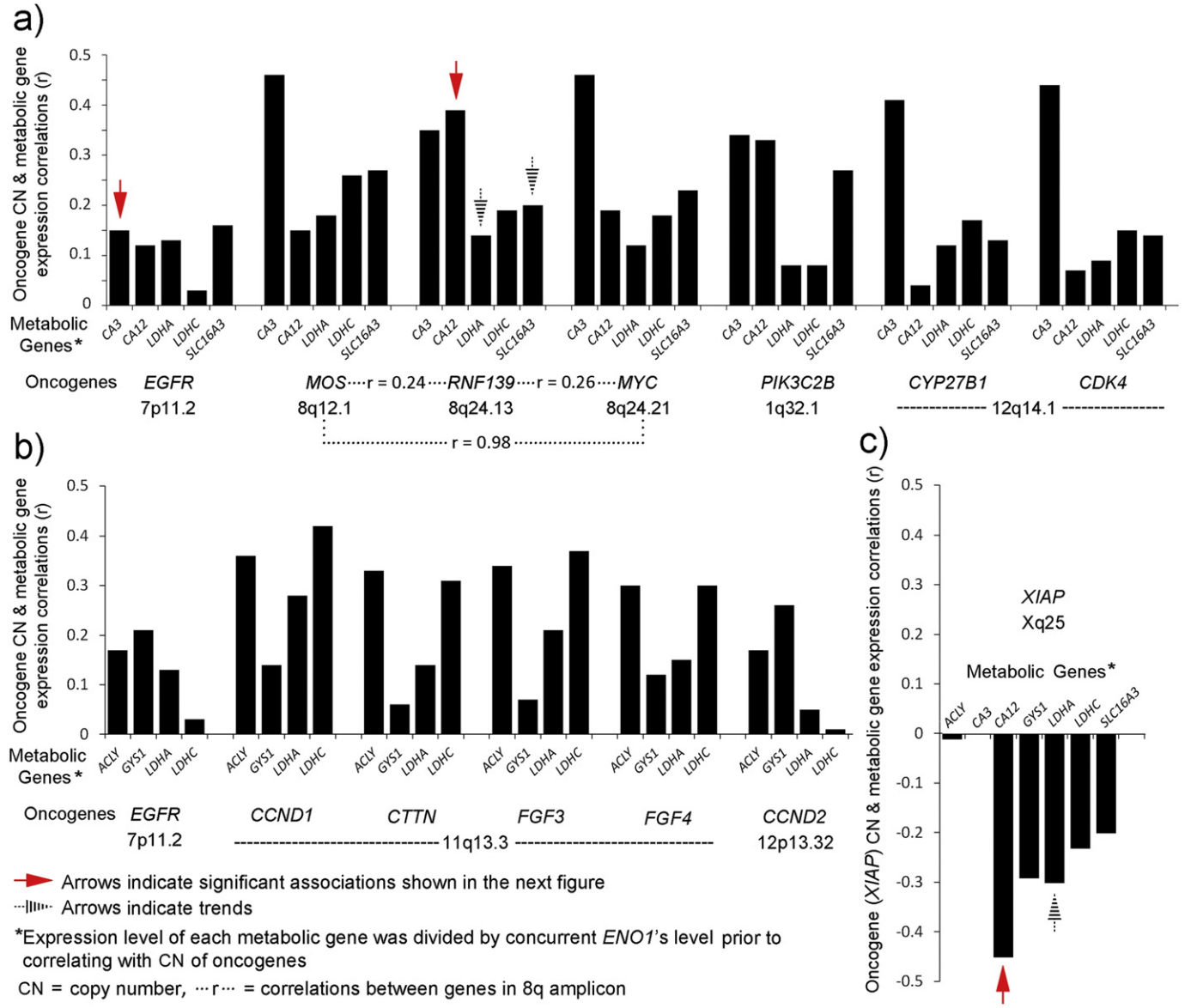

Fig. 6. Patterns of functional relevance in the correlations between metabolic genes and oncogenes. (a) A pattern attributed to genes whose expressions protect glycolysis in acidic conditions, possibly to supra-physiologic limits. Positive correlations of the *ENO1* transformed expressions of metabolic genes (*CA3*, *CA12*, *LDHA*, *LDHC*, and *SLC16A3*(or *MCT4*)) occurred with CN of oncogenes (*EGFR*, *MOS*, *RNF139*, *MYC*, *PIK3C2B*, *CYP27B1*, and *CDK4*). Those supported by significant associations (Wilcoxon Rank Sum, Section 3.6) are indicated by solid red arrows and trends by black striped arrows. Complexity within a potential 8q amplicon is indicated by strong correlation ($r = 0.98$) between *MOS* and *MYC* but weaker correlations between each of them and intervening *RNF139*. (b) A pattern attributed to non-aerobic glycolysis operating in intermittent avascular conditions based on previous studies of glycolytic-dependent glioblastoma cell migration [9,11], involving *ENO1* transformed expressions of metabolic genes, *ACLY*, *GYS1*, *LDHA*, and *LDHA*, was identified by shared positive correlations with CN of oncogenes, *EGFR*, *CCND1*, *CTTN*, *FGF3*, *FGF4*, and *CCND2*. (c) The CN gain of *XIAP* revealed an opposing pattern for metabolic genes' expressions. The significant association (Wilcoxon Rank Sum, Section 3.6) and a trend are indicated by the solid red and striped black arrows, respectively.

anoxic stress for 4 h led to increased levels of CAIII, among other isoforms, in the cerebral cortex, hippocampus, cerebellum, and retina of piglets [36]. Interestingly, in hepatoma cells overexpression of *CA3* by transfection resulted in increased extracellular acidification, anchorage-independent growth and invasiveness with elevated focal adhesion kinase (FAK) and Src activity [37]. Increased *EGFRvIII* expression has been associated with protein levels of CAIII and poor survival in glioblastomas [38]. Previously, we detected four phosphorylated tyrosine (pY) residues (Y845, Y992, Y1045, and Y1068) in EGFR within pseudopodia of migrating glioblastoma cells [39]. The pseudopodia constitute a relatively glycolytic subcellular domain compared to whole cells [1]. Others have proposed that EGFR's "Y/pY fingerprints" defined in time courses may "encode" acid–base disturbances [40]. This study of glioblastomas showed that CN gains in *EGFR* of 2.00-fold or greater significantly associated with expression levels of *CA3*, transformed by concurrent levels of *ENO1*. Thus, the metabolic role played by carbonic anhydrase III in glioblastomas is possibly influenced by effects due to gains in CN of *EGFR* and its signaling on *CA3*'s expression levels.

The other significant associations found in this study were for CN of oncogenes and gender with *CA12* that encodes the transmembrane carbonic anhydrase, CAXII. Gains in CN of *RNF139*, lack of gains in *XIAP*, and male gender associated significantly with expression of *CA12* in this study's glioblastomas. Interestingly, the two amplified oncogenes, *RNF139* and *XIAP*, that had opposing associations with expression of *CA12*, both encode RING proteins that are E3 ubiquitin ligases [41–44].

Previously CAXII has been found in multiple types of tumors with expression results in some suggesting a malignant role. Immunohistochemistry demonstrated CAXII in oncocytomas and clear-cell carcinomas of the kidneys [45] and ovarian carcinomas [46]. In assays of

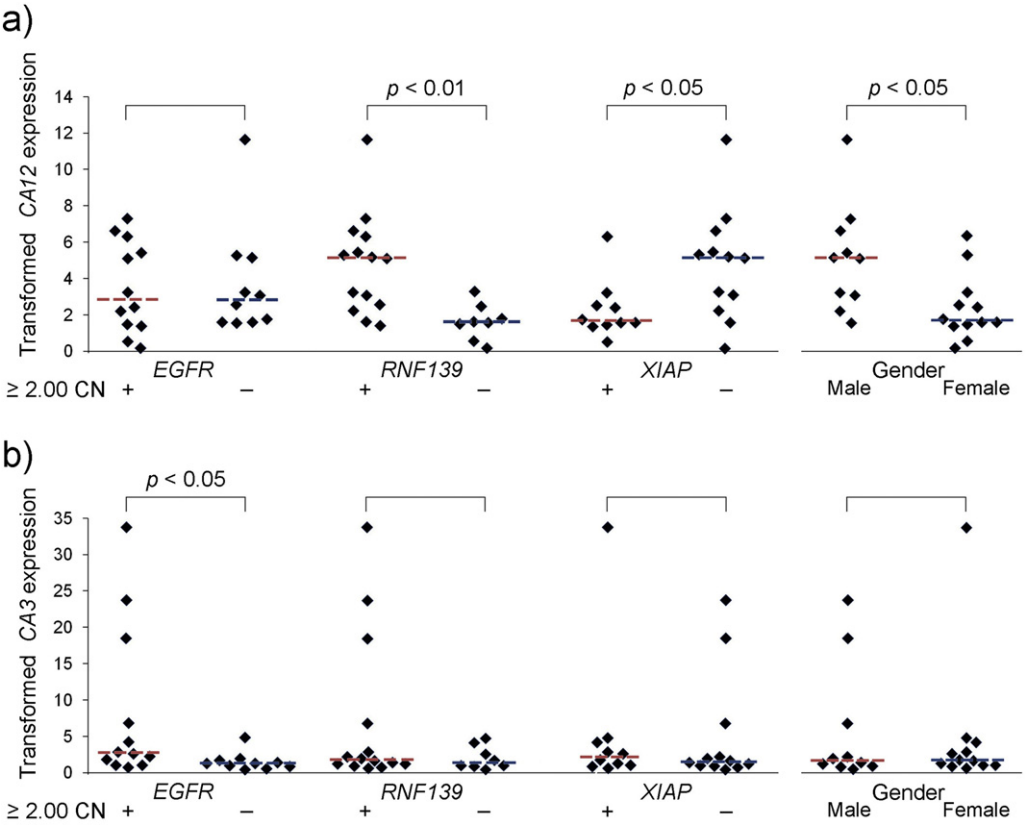

Fig. 7. Expressions of carbonic anhydrase genes, *CA3* and *CA12*, transformed by *ENO1*, associated significantly in Wilcoxon Rank Sum analyses with CN changes and gender in glioblastomas. (a) Transformed *CA12* expression associated significantly with CN gains of *RNF139* that were 2.00-fold or greater, lack of a 2.00-fold or greater CN gain in *XIAP*, and with male gender. (b) Transformed *CA3* expression associated significantly with CN gains of *EGFR* that were 2.00-fold or greater. The red and blue dashed lines among the data points indicate the medians for each data group as indicated.

hypoxic colon adenocarcinoma cells, silencing of *CA9* alone led to a 40% reduction in xenograft tumor volume with accompanying up-regulation of *CA12* mRNA levels, whereas silencing of both *CA9* and *CA12* led to a greater (85%) reduction in tumor volume. Also, when *CA9* was silenced in vivo, there was an increase in the amount of CAXII shown with immunostaining [47]. Gene knockdown studies of *CA12* in breast carcinoma cells decreased their invasiveness that was restored by overexpressing *CA12* [48]. Protein expression of CAXII in oral squamous carcinoma has been associated with more advanced clinical stages, larger tumor size, recurrence, and poorer prognosis [49]. Both *CA9*/CAIX and *CA12*/CAXII have been studied in lung adenocarcinoma cell lines [50]. In colon carcinoma, CAXII was upregulated on the surfaces of chemoresistant cells [51]. In diffuse astrocytomas, two forms of CAXII occur derived from alternative splicing. Immunoreactivity for CAXII was found in 98% of 363 astrocytomas and its increased expression correlated with higher World Health Organization (WHO) grade, older age, and poorer prognosis independent of patient age and WHO grade [52]. Our selection of *CA12* as a gene from the large carbonic anhydrase family to study was based partly on significantly poorer patient survival at high levels of expression in glioblastomas found in the REMBRANDT database during 2007–2008 [8].

Statistically significant associations found in our study included greater expression of *CA12* (transformed by *ENO1*) occurring with 2.00-fold or greater CN of *RNF139*, previously known as *TRC8* for "translocation in renal carcinoma". *RNF139* occurs as a chromosomal translocation, t(3;8)(p14.2;q24.1) in some familial renal cancers [53–55] and another *RNF139* translocation, t(8;22)(q24.13;q11.21) has been reported in a dysgerminoma [56]. In clear cell renal carcinomas, *RNF139* has been thought to act as a tumor suppressor [41,42,57–59]. However, *RNF139* is expressed in non-renal tissues, including brain [60], and gains in the expression and CN of *RNF139* have recently been noted in studies that include non-renal tumors. In a refractory cancer gene set interaction network (113 cancer patient samples) annotated with tissue type specificity, *RNF139* was overexpressed in 9 of 16 pancreas samples, $p = 0.0085$, compared to normal tissue samples [61]. Also, *RNF139* was one of three predicted driver genes in cancer shared among breast, melanoma, and liver cancers based on a computational method that analyzed CN aberrations in human cancer genomes [62]. A study on primary oral tumor samples and nearby tumor-free tissues identified *RNF139* among a group of 14 genes exhibiting CN gains out of 133 cancer-related genes [63]. Increases in *RNF139* gene expression were found in comparisons of Barrett esophagus (precancerous) and esophageal adenocarcinomas with normal esophagus [64]. Our study suggests that CN gains in *RNF139* found in glioblastomas are associated with the increased expression of *CA12*.

Another statistically significant association for an oncogene in our study occurred for the greater expression of *CA12* (transformed by *ENO1*) when CN of *XIAP* (*X-linked inhibitor of apoptosis*, previously known as *BIRC4*) was less than 2.00-fold. In other words, there was a negative correlation with CN gains in *XIAP* for increased expression of *CA12*. Others have found XIAP and two other inhibitors of apoptosis in twelve malignant glioma cell lines [65]. Although XIAP is known as an endogenous repressor of the terminal caspase cascade in apoptosis, it may also be involved in other activities, including modulation of signal transduction and protein ubiquitination. XIAP is synthesized during conditions of stress that inhibit protein synthesis [66]. When *XIAP* is translated by a mechanism involving an internal ribosome entry site (IRES), interactions of XIAP IRES with MDM2 may affect stabilization of itself and MDM2. Interestingly, because XIAP can induce autophagy, it can have an antitumor effect in early tumorigenesis in contrast to being an aid for tumor survival in stressful conditions. Therefore, XIAP's role in tumors has been proposed to be contextual [67]. Mutational loss

of XIAP is responsible for X-linked lymphoproliferative syndrome type 2 [68,69].

Although *XIAP*'s CN could potentially be influenced by X chromosomal inactivation, instead, its CN is normally determined by the number of X chromosomes. One copy of *XIAP* in males and two in females, with no evidence of a CN variation, were found in 400 individuals tested with quantitative PCR in a recent asthma study [13]. Also, differences in response to cerebral ischemia in stroke according to gender have been attributed to XIAP's correspondence to chromosomal dosage [70]. In regard to tumors, increased XIAP demonstrated with immunohistochemistry in hepatocellular carcinoma specimens was associated with small tumor size, early tumor stage, and better relapse-free and overall survival [71]. Also, in a mouse model that demonstrates progression to malignant peripheral nerve sheath tumors (MPNST) from neurofibromas, a loss in CN for *XIAP* was found in early passage cell lines established from the MPNSTs [72]. Accordingly, the negative correlation and significant association for lack of *XIAP* gains with expression of *CA12* in our study suggests that it may regulate expression of *CA12* to control acidity in tumors. However, this relationship is complex in that there are also reports of several types of tumors, including gliomas, where targeting *XIAP* has been suggested for treatment purposes [73–76].

Regulation of pH is an essential requirement for life in that protein interactions are very sensitive to pH, such as those of phosphofructokinase. Vulnerabilities of phosphofructokinase and other glycolytic enzymes are being considered as important treatment targets [77]. The access of tumors to the bicarbonate buffer system in the bloodstream is possibly optimized by oncogenes (Fig. 8). This study identified CN gains of *EGFR* and *RNF139*, male gender, and lack of *XIAP*'s CN gains as having significant associations with expressions of carbonic anhydrases that catalyze interconversions of the bicarbonate buffer's components within and around tumor cells. Gains in CN for *EGFR* significantly associated with expression of *CA3*, that encodes an intracellular carbonic anhydrase, CAIII. Gains in *RNF139* significantly associated with *CA12*'s expression that encodes CAXII, whose activity is extracellular. The proposed effects of gains in CN of the three oncogenes are illustrated (Fig. 8, bottom panel). Gender and lack of CN gains for *XIAP* may be factors in tumor biology. The gains in CN for *EGFR* and *RNF139* within tumors may aid tumors metabolically and potentially can serve as therapeutic targets to counteract non-physiologic pH changes in tumors.

Also, in tumor cells there is a functional relationship between lactate dehydrogenases and carbonic anhydrases in that with increasing ATP via lactate production, there is higher demand for pH regulation mediated by carbonic anhydrases. Accordingly, in this study there was a trend for CN gains of *RNF139* to associate with expression of *LDHA*. CN gains of *RNF139* also showed a trend for associating with expression of *SLC16A3* (also known as *MCT4*) that extrudes lactic acid from cells. Additionally, male gender and the lack of CN gains for *XIAP* trended positively with expression of *LDHA*. For *LDHC*, a Fisher's Exact test revealed a significant association for its increased expression with any 3.00-fold or greater oncogene CN gain in this study.

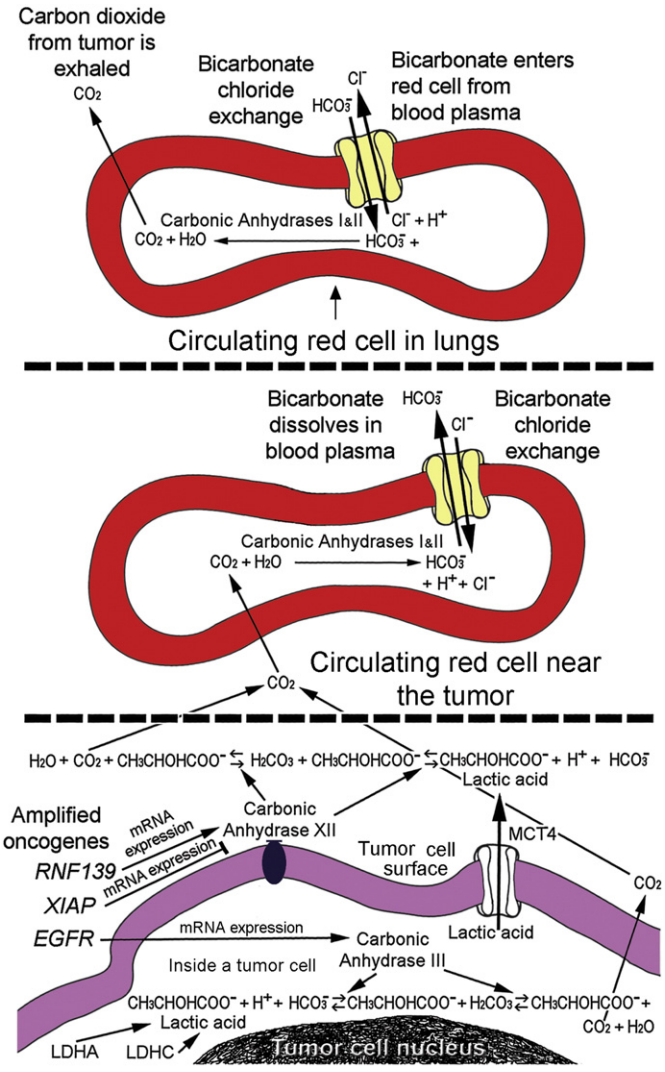

Fig. 8. Roles for amplified oncogenes, *EGFR*, *RNF139*, and *XIAP*, to control pH via access to the systemic bicarbonate buffer system in aiding glioblastoma cells. Red cells and plasma in the blood stream (upper panels) remove carbons via CO_2 that is exhaled in the lungs. Transport of CO_2/HCO_3^- occurs in a relay fashion within the circulation. Large amounts of bicarbonate in the bloodstream buffer protons and levels are maintained via recycling in the kidneys where the protons carried by bicarbonate are expelled. Amplified *EGFR* and *RNF139* may enhance expression of *CA3* and *CA12*, respectively, to increase encoded tumor carbonic anhydrases (lower panel). In contrast, *XIAP* may reduce expression of *CA12*. Lactic acid membrane transporter, MCT4, is encoded by *SLC16A3*. The edge of a tumor cell is in the lowest panel. Red cells are depicted with reactions derived from other diagrams [78–80]. H^+ ions (protons) from ATP breakdown during anaerobic metabolism involving lactic acid is a process explained elsewhere [81].

5. Conclusions

The sensitivity of PCR methodologies, selection of metabolic genes using functional relevance and REMBRANDT data, inclusion of many known oncogenes to screen, and using *ENO1* transformation to adjust for tumor heterogeneity and obtain supra-glycolytic metabolic gene expression levels were contributing factors that led to the identification of significant associations between oncogene CN changes and metabolic gene expression levels in this study. Regulation of pH emerged as a potential oncogene-mediated advantage for tumor cells so that roles for oncogenes in controlling tumor pH are compelling to consider in future treatment regimens. Slight increases in expression of carbonic anhydrases with rapid catalytic rates due to oncogene CN changes may provide dramatic advantages for tumors. Our findings suggest that oncogenes in glioblastomas increase utilization of the body's vast, systemic bicarbonate buffering system to aberrantly control pH. Identification of participating oncogenes may identify functional subgroups among glioblastomas in larger studies. These oncogenes, when amplified, may be culprits that enable malignant metabolism to robustly energize tumor cells that outcompete normal cells with clinically important prognostic and therapeutic implications.

Disclosure summary

The authors declare no conflict of interest.

Transparency document

The Transparency document associated with this article can be found, in online version.

Acknowledgments

We thank The Pittsburgh Foundation's Walter L. Copeland Fund for Cranial Research (D2006-0379) and Louisiana State University Health Sciences Center in Shreveport Grant-in-Aid for funding. Technical assistance, including usage of equipment, was graciously provided as needed by Molecular Diagnostic Laboratories in the Departments of Pathology at Louisiana State University Health, Shreveport, LA, and at the University of Pittsburgh Medical Center, Pittsburgh, PA. We are especially grateful for the contributions of Jeffrey A. Kant, MD, PhD, former director of the Molecular Diagnostics Laboratory, Department of Pathology, University of Pittsburgh, Pittsburgh, PA, now deceased, to many of the early steps taken in determining how this study progressed and evolved.

References

[1] M.E. Beckner, X. Chen, J. An, B.W. Day, I.F. Pollack, Proteomic characterization of harvested pseudopodia with differential gel electrophoresis and specific antibodies, Lab. Invest. 85 (2005) 316–327.
[2] F.L. Muller, S. Colla, E. Aquilanti, V. Manzo, G. Genovese, J. Lee, D. Eisenson, R. Narurkar, P. Deng, L. Nezi, M. Lee, B. Hu, J. Hu, et al., Passenger deletions generate therapeutic vulnerabilities in cancer, Nature 488 (2012) 337–342, http://dx.doi.org/10.1038/nature11331.
[3] O. Warburg, On the origin of cancer cells, Science 123 (1956) 309–314.
[4] N. Laiken, D.D. Fanestil, Acid–base Balance and Regulation of H^+ Excretion *in* Best and Taylor's Physiological Basis of Medical Practice, 12th ed. West JB ed., Williams & Wilkins, Baltimore, MD, 1990 486–493 Chapter 32.
[5] L.A. Skelton, W.F. Boron, Y. Zhou, Acid–base transport by the renal proximal tubule, J. Nephrol. 23 (Suppl. 16) (2010) S4–S18.
[6] L.N. Truong, S. Patil, S.S. Martin, J.F. LeBlanc, A. Nanda, M.L. Nordberg, M.E. Beckner, Rapid detection of high-level oncogene amplifications in ultrasonic surgical aspirations of brain tumors, Diagn. Pathol. 7 (2012) 66, http://dx.doi.org/10.1186/1746-1596-7-66.
[7] M.E. Beckner, R. Sampath, A.B. Flowers, K. Katira, D. D'Souza, S. Patil, R.B. Patel, M.L. Nordberg, A. Nanda, Low-level amplification of oncogenes correlates inversely with age for patients with nontypical meningiomas, World Neurosurg. 79 (2013) 313–319, http://dx.doi.org/10.1016/j.wneu.2011.08.023.
[8] Repository of Molecular Brain Neoplasia Database (REMBRANDT) v1.52 and earlier versions, generated and maintained by the NCI and NINDS at NIHAvailable at: http://rembrandt.nci.nih.govFebruary, 2008 (data (93 glioblastomas available)).
[9] M.E. Beckner, W. Fellows-Mayle, Z. Zhang, N.R. Agostino, J.A. Kant, B.W. Day, I.F. Pollack, Identification of ATP citrate lyase as a positive regulator of glycolytic function in glioblastomas, Int. J. Cancer 126 (2010) 2282–2295, http://dx.doi.org/10.1002/ijc.24918.
[10] M.E. Beckner, Co-amplified oncogenes in glioblastomas, in: M.F. Bezerra, C.R. Alves (Eds.), Glioblastoma: Risk Factors, Diagnosis and Treatment Options, Nova Science Publishers, Inc., Hauppauge, NY 2012, pp. 101–115 Chapter 4.
[11] M.E. Beckner, G.T. Gobbel, R. Abounader, F. Burovic, N.R. Agostino, J. Laterra, I.F. Pollack, Glycolytic glioma cells with active glycogen synthase are sensitive to PTEN and inhibitors of PI3K and gluconeogenesis, Lab. Invest. 85 (2005) 1457–1470.
[12] M.E. Beckner, M.L. Stracke, L.A. Liotta, E. Schiffmann, Glycolysis as primary energy source in tumor cell chemotaxis, J. Natl. Cancer Inst. 82 (1990) 1836–1840.
[13] E. Roscioli, R. Hamon, R.E. Ruffin, P. Zalewski, J. Grant, S. Lester, X-linked inhibitor of apoptosis single nucleotide polymorphisms and copy number variation are not risk factors for asthma, Respirology 18 (2013) 697–703, http://dx.doi.org/10.1111/resp.12065.
[14] U. Schindler, E. Betz, Influence of severe hypercapnia upon cerebral cortical metabolism, CSF electrolyte concentrations and EEG in the cat, Bull. Eur. Physiopathol. Respir. 12 (1976) 277–284.
[15] M.J. Achs, D. Garfinkel, Computer simulation of energy metabolism in acidotic cardiac ischemia, Am. J. Physiol. 242 (1982) R533–R544.
[16] P.J. Mulquiney, P.W. Kuchel, Model of the pH-dependence of the concentrations of complexes involving metabolites, haemoglobin and magnesium ions in the human erythrocyte, Eur. J. Biochem. 245 (1997) 71–83.
[17] T. Costa Leite, D. Da Silva, R. Guimaraes Coelho, P. Zancan, M. Sola-Penna, Lactate favours the dissociation of skeletal muscle 6-phosphofructo-1-kinase tetramers down-regulating the enzyme and muscle glycolysis, Biochem. J. 408 (2007) 123–130.
[18] A. De Milito, S. Fais, Proton pump inhibitors may reduce tumour resistance, Expert. Opin. Pharmacother. 6 (2005) 1049–1054.
[19] S. Fais, A. De Milito, H. You, W. Qin, Targeting vacuolar H+-ATPases as a new strategy against cancer, Cancer Res. 67 (2007) 10627–10630.
[20] A. Hulikova, Harris AI, Vaughan-Jones RD, and Swietach P. Acid-extrusion from tissue: the interplay between membrane transporters and pH buffers, Curr. Pharm. Des. 18 (2012) 1331–1337.
[21] C. Daniel, C. Bell, C. Burton, S. Harguindey, S.J. Reshkin, C. Rauch, The role of proton dynamics in the development and maintenance of multidrug resistance in cancer, Biochim. Biophys. Acta 2013 (1832) 606–617, http://dx.doi.org/10.1016/j.bbadis.2013.01.020.
[22] H.M. Becker, M. Klier, J.W. Deitmer, Carbonic anhydrases and their interplay with acid/base-coupled membrane transporters, Subcell. Biochem. 75 (2014) 105–134, http://dx.doi.org/10.1007/978–94-007-7359-2_7.
[23] A. Shiozaki, D. Ichikawa, E. Otsuji, Y. Marunaka, Cellular physiological approach for treatment of gastric cancer, World J. Gastroenterol. 20 (2014) 11560–11566, http://dx.doi.org/10.3748/wjg.v20.i33.11560.
[24] E.P. Spugnini, P. Sonveaux, C. Stock, M. Perez-Sayans, A. De Milito, S. Avnet, A.G. Garcia, S. Harguindey, S. Fais, Proton channels and exchangers in cancer, Biochim. Biophys. Acta (Oct 20 2014)http://dx.doi.org/10.1016/j.bbamem.2014.10.015 (pii: S0005-2736(14)00350–2. [Epub ahead of print]).
[25] P. Swietach, R.D. Vaughan-Jones, A.L. Harris, A. Hulikova, The chemistry, physiology and pathology of pH in cancer, Philos. Trans. R. Soc. Lond. Ser. B Biol. Sci. 369 (2014) 20130099, http://dx.doi.org/10.1098/rstb.2013.0099.
[26] S. Lindskog, Structure and mechanism of carbonic anhydrase, Pharmacol. Ther. 74 (1997) 1–20.
[27] S.R. Paranawithana, C. Tu, P.J. Laipis, D.N. Silverman, Enhancement of the catalytic activity of carbonic anhydrase III by phosphates, J. Biol. Chem. 265 (1990) 22270–22274.
[28] D.A. Jewell, C. Tu, S.R. Paranawithana, S.M. Tanhauser, P.V. LoGrasso, P.J. Laipis, D.N. Silverman, Enhancement of the catalytic properties of human carbonic anhydrase III by site-directed mutagenesis, Biochemistry 30 (1991) 1484–1490.
[29] P.V. LoGrasso, C. Tu, D.A. Jewell, G.C. Wynns, P.J. Laipis, D.N. Silverman, Catalytic enhancement of human carbonic anhydrase III by replacement of phenylalanine-198 with leucine, Biochemistry 30 (1991) 8463–8470.
[30] H.K. Vaananen, H. Autio-Harmainen, Carbonic anhydrase III: a new histochemical marker for myoepithelial cells, J. Histochem. Cytochem. 35 (1987) 683–686.
[31] S. Tweedie, K. Morrison, J. Charlton, Y.H. Edwards, CAIII a marker for early myogenesis: analysis of expression in cultured myogenic cells, Somat. Cell Mol. Genet. 17 (1991) 215–228.
[32] Y.H. Edwards, S. Tweedie, N. Lowe, G. Lyons, Carbonic anhydrase 3 (CA3), a mesodermal marker, Symp. Soc. Exp. Biol. 46 (1992) 273–283.
[33] J. Zoll, E. Ponsot, S. Dufour, S. Doutreleau, R. Ventura-Clapier, M. Vogt, H. Hoppeler, R. Richard, M. Fluck, Exercise training in normobaric hypoxia in endurance runners. III. Muscular adjustments of selected gene transcripts, J. Appl. Physiol. 100 (2006) 1258–1266.
[34] R. Faiss, B. Leger, J.-M. Vesin, P.-E. Fournier, Y. Eggel, O. Deriaz, G.P. Millet, Significant molecular and systemic adaptations after repeated sprint training in hypoxia, PLoS One 8 (2013), e56522http://dx.doi.org/10.1371/journal.pone.0056522.
[35] L. Staunton, M. Zweyer, D. Swandulla, K. Ohlendieck, Mass spectrometry-based proteomic analysis of middle-aged vs. aged vastus lateralis reveals increased levels of carbonic anhydrase isoform 3 in senescent human skeletal muscle, Int. J. Mol. Med. 30 (2012) 723–733, http://dx.doi.org/10.3892/ijmm.2012.1056.
[36] A. Nogradi, F. Domoki, R. Degi, S. Borda, M. Pakaski, A. Szabo, F. Bari, Up-regulation of cerebral carbonic anhydrase by anoxic stress in piglets, J. Neurochem. 85 (2003) 843–850.
[37] H.Y. Dai, C.C. Hong, S.C. Liang, M.D. Yan, G.M. Lai, A.L. Cheng, S.E. Chuang, Carbonic anhydrase III promotes transformation and invasion capability in hepatoma cells through FAK signaling pathway, Mol. Carcinog. 47 (2008) 956–963, http://dx.doi.org/10.1002/mc.20448.
[38] H. Johnson, A.M. Del Rosario, B.D. Bryson, M.A. Schroeder, J.N. Sarkaria, F.M. White, Molecular characterization of EGFR and EGFRvIII signaling networks in human glioblastoma tumor xenografts, Mol. Cell. Proteomics 11 (2012) 1724–1740, http://dx.doi.org/10.1074/mcp.M112.019984.
[39] M.E. Beckner, S.A. Aznavoorian-Cheshire, I.F. Pollack, Reactivity for activated epidermal growth factor receptor is demonstrated in the pseudopodia of migratory glioma cells, Proc. Am. Assoc. Cancer Res. 46 (2005) 1327, A5641.
[40] L.A. Skelton, W.F. Boron, Effect of acute acid–base disturbances on ErbB1/2 tyrosine phosphorylation in rabbit renal proximal tubules, Am. J. Physiol. Ren. Physiol. 305 (2013) F1747–F1764, http://dx.doi.org/10.1152/ajprenal.00307.2013.
[41] A. Brauweiler, K.L. Lorick, J.P. Lee, Y.C. Tsai, D. Chan, A.M. Weissman, H.A. Drabkin, R.M. Gemmill, RING-dependent tumor suppression and G2/M arrest induced by the TRC8 hereditary kidney cancer gene, Oncogene 26 (2007) 2263–2271.
[42] J.P. Lee, A. Brauweiler, M. Rudolph, J.E. Hooper, H.A. Drabkin, R.M. Gemmill, The TRC8 ubiquitin ligase is sterol regulated and interacts with lipid and protein biosynthetic pathways, Mol. Cancer Res. 8 (2010) 93–106, http://dx.doi.org/10.1158/1541-7786.MCR-08-0491.
[43] S. Galban, C.S. Duckett, XIAP as a ubiquitin ligase in cellular signaling, Cell Death Differ. 17 (2010) 54–60, http://dx.doi.org/10.1038/cdd.2009.81.
[44] Y. Nakatani, T. Kleffmann, K. Linke, S.M. Condon, M.G. Hinds, C.L. Day, Regulation of ubiquitin transfer by XIAP, a dimeric RING E3 ligase, Biochem. J. 450 (2013) 629–638, http://dx.doi.org/10.1042/BJ20121702.
[45] S. Parkkila, A.K. Parkkila, J. Saarnio, J. Kivela, T.J. Karttunen, K. Kaunisto, A. Waheed, W.S. Sly, O. Tureci, I. Virtanen, H. Rajaniemi, Expression of the membrane-associated carbonic anhydrase isozyme XII in the human kidney and renal tumors, J. Histochem. Cytochem. 48 (2000) 1601–1608.
[46] P. Hynninen, L. Vaskivuo, J. Saarnio, H. Haapasalo, J. Kivela, S. Pastorekova, J. Pastorek, A. Waheed, W.S. Sly, U. Puistola, S. Parkkila, Expression of transmembrane carbonic anhydrase IX and XII in ovarian tumours, Histopathology 49 (2006) 594–602.
[47] J. Chiche, K. Ilc, J. Laferriere, E. Trottier, F. Dayan, N.M. Mazure, M.C. Brahimi-Horn, J. Pouyssegur, Hypoxia-inducible carbonic anhydrase IX and XII promote tumor cell growth by counteracting acidosis through the regulation of the intracellular pH, Cancer Res. 69 (2009) 358–368, http://dx.doi.org/10.1158/0008-5472.CAN-08-2470.
[48] M.J. Hsieh, K.S. Chen, H.L. Chiou, Y.S. Hsieh, Carbonic anhydrase XII promotes invasion and migration ability of MDA-MB-231 breast cancer cells through the p38 MAPK signaling pathway, Eur. J. Cell Biol. 89 (2010) 598–606, http://dx.doi.org/10.1016/j.ejcb.2010.03.004.
[49] M.H. Chien, T.H. Ying, Y.H. Hsieh, C.H. Lin, C.H. Shih, L.H. Wei, S.F. Yang, Tumor-associated carbonic anhydrase XII is linked to the growth of primary oral squamous cell carcinoma and its poor prognosis, Oral Oncol. 48 (2011) 417–423, http://dx.doi.org/10.1016/j.oraloncology.2011.11.015.

[50] M. Ilie, V. Hofman, J. Zangari, J. Chiche, J. Mouroux, N.M. Mazure, J. Pouyssegur, P. Brest, P. Hofman, Response of CAIX and CAXII to *in vitro* re-oxygenation and clinical significance of the combined expression in NSCLC patients, Lung Cancer 82 (2013) 16–23, http://dx.doi.org/10.1016/j.lungcan.2013.07.005.
[51] J. Kopecka, I. Campia, A. Jacobs, A.P. Frei, D. Ghigo, B. Wollscheid, C. Riganti, Carbonic anhydrase XII is a new therapeutic target to overcome chemoresistance in cancer cells, Oncotarget 6 (2015) 6776–6793.
[52] J. Haapasalo, M. Hilvo, K. Nordfors, H. Haapasalo, S. Parkkila, A. Hyrskyluoto, I. Rantala, A. Waheed, W.S. Sly, S. Pastorekova, J. Pastorek, A.-K. Parkkila, Identification of an alternatively spliced isoform of carbonic anhydrase XII in diffusely infiltrating astrocytic gliomas, Neuro-Oncology 10 (2008) 131–138, http://dx.doi.org/10.1215/15228517-2007-065.
[53] R.M. Gemmill, J.D. West, F. Boldog, N. Tanaka, L.J. Robinson, D.I. Smith, F. Li, H.A. Drabkin, The hereditary renal cell carcinoma 3;8 translocation fuses *FHIT* to a patched-related gene, *TRC8*, Proc. Natl. Acad. Sci. U. S. A. 95 (1998) 9572–9577.
[54] K.S. Poland, M. Azim, M. Folsom, R. Goldfarb, R. Naeem, C. Korch, H.A. Drabkin, R.M. Gemmill, S.E. Plon, A constitutional balanced t(3;8)(p14;q24.1) translocation results in disruption of the TRC8 gene and predisposition to clear cell renal cell carcinoma, Genes Chromosomes Cancer 46 (2007) 805–812.
[55] T. Kato, C.P. Franconi, M.B. Sheridan, A.M. Hacker, H. Inagakai, T.W. Glover, M.F. Arlt, H.A. Drabkin, R.M. Gemmill, H. Kurahashi, B.S. Emanuel, Analysis of the t(3;8) of hereditary renal cell carcinoma: a palindrome-mediated translocation, Cancer Genet. 207 (2014) 133–140, http://dx.doi.org/10.1016/j.cancergen.2014.03.004.
[56] S. Gimelli, S. Beri, H.A. Drabkin, C. Gambini, A. Gregorio, P. Fiorio, O. Zuffardi, R.M. Gemmill, R. Giorda, G. Gimelli, The tumor suppressor gene TRC8/RNF139 is disrupted by a constitutional balanced translocation t(8;22)(q24.13;q11.21) in a young girl with dysgerminoma, Mol. Cancer 8 (2009) 52, http://dx.doi.org/10.1186/1476-4598-8-52.
[57] H.A. Drabkin, R.M. Gemmill, Obesity, cholesterol, and clear-cell renal cell carcinoma (RCC), Adv. Cancer Res. 107 (2010) 39–56, http://dx.doi.org/10.1016/S0065-230X(10)07002-8.
[58] H.A. Drabkin, R.M. Gemmill, Cholesterol and the development of clear-cell renal carcinoma, Curr. Opin. Pharmacol. 12 (2012) 742–750, http://dx.doi.org/10.1016/j.coph.2012.08.002.
[59] P.H. Lin, W.M. Lan, L.Y. Chau, TRC8 suppresses tumorigenesis through targeting heme oxygenase-1 for ubiquitination and degradation, Oncogene 32 (2013) 2325–2334, http://dx.doi.org/10.1038/onc.2012.244.
[60] D. Charytoniuk, B. Porcel, J. Rodriguez Gomez, H. Faure, M. Ruat, E. Traiffort, Sonic hedgehog signaling in the developing and adult brain, J. Physiol. Paris 96 (2002) 9–16.
[61] S. Jung, M. Verdicchio, J. Kiefer, D. Von Hoff, M. Berens, M. Bittner, S. Kim, Learning contextual gene set interaction networks of cancer with condition specificity, BMC Genomics 14 (2013) 110, http://dx.doi.org/10.1186/1471-2164-14-110.
[62] Y. Chen, J. Hao, W. Jiang, T. He, X. Zhang, T. Jiang, R. Jiang, Identifying potential cancer driver genes by genomic data integration, Sci. Rep. 3 (2013) 3538, http://dx.doi.org/10.1038/srepo3538.
[63] I.P. Ribeiro, F. Marques, F. Caramelo, J. Pereira, M. Patricio, H. Prazeres, J. Ferrao, M.J. Juliao, M. Castelo-Branco, J.B. de Melo, I.P. Baptista, I.M. Carreira, Genetic gains and losses in oral squamous cell carcinoma: impact on clinical management, Cell. Oncol. (Dordr) 37 (2014) 29–39, http://dx.doi.org/10.1007/S13402-013-0161-5.
[64] X.W. Wang, W. Wei, W.Q. Wang, X.Y. Zhao, H. Guo, D.C. Fand, RING finger proteins are involved in the progression of Barrett esophagus to esophageal adenocarcinoma: a preliminary study, Gut Liver 8 (2014) 487–494, http://dx.doi.org/10.5009/gnl13133.
[65] B. Wagenknecht, T. Glaser, U. Naumann, S. Kugler, S. Isenmann, M. Bahr, R. Korneluk, P. Liston, M. Weller, Expression and biological activity of X-linked inhibitor of apoptosis (XIAP) in human malignant glioma, Cell Death Differ. 6 (1999) 370–376.
[66] M. Holcik, H. Gibson, R.G. Korneluk, XIAP: apoptotic brake and promising therapeutic target, Apoptosis 6 (2001) 253–261.
[67] T. Liu, H. Zhang, J. Xiong, S. Yi, L. Gu, M. Zhou, Inhibition of MDM2 homodimerization by XIAP IRES stabilizes MDM2, influencing cancer cell survival, Mol. Cancer 14 (2015) 65, http://dx.doi.org/10.1186/s12943-015-0334-0.
[68] C. Aguilar, S. Latour, X-linked inhibitor of apoptosis protein deficiency: more than an X-linked lymphoproliferative syndrome, J. Clin. Immunol. 35 (2015) 331–338, http://dx.doi.org/10.1007/s10875-015-0141-9.
[69] M. Dziadzio, S. Ammann, C. Canning, F. Boyle, A. Hassan, C. Cale, M. Elawad, B.K. Fiil, M. Gyrd-Hansen, U. Salzer, Speckmann c, and Grimbacher B. Symptomatic males and female carriers in a large Caucasian kindred with XIAP deficiency, J. Clin. Immunol. 35 (2015) 439–444, http://dx.doi.org/10.1007/s10875-015-0166-0.
[70] C. Siegel, J. Li, F. Liu, S.E. Benashski, L.D. McCullough, miR-23a regulation of X-linked inhibitor of apoptosis (XIAP) contributes to sex differences in the response to cerebral ischemia, Proc. Natl. Acad. Sci. U. S. A. 108 (2011) 11662–11667, http://dx.doi.org/10.1073/pnas.1102635108.
[71] W.Y. Wu, H. Kim, C.L. Zhang, X.L. Meng, Z.S. Wu, Clinical significance of autophagic protein LC3 levels and its correlation with XIAP expression in hepatocellular carcinoma, Med. Oncol. 31 (2014) 108, http://dx.doi.org/10.1007/s12032-014-0108-3.
[72] S.J. Kazmi, S.J. Byer, J.M. Eckert, A.N. Turk, R.P.H. Huijbregts, N.M. Brossier, W.E. Grizzle, F.M. Mikhail, K.A. Roth, S.L. Carroll, Transgenic mice overexpression neuregulin-1 model neurofibroma-malignant peripheral nerve sheath tumor progression and implicate chromosomal copy number variations in tumorigenesis, Am. J. Pathol. 182 (2013) 646–667, http://dx.doi.org/10.1016/j.ajpath.2012.11.017.
[73] A. Hosni-Ahmed, M. Sims, T.S. Jones, R. Patil, S. Patil, H. Abdelsamed, C.R. Yates, D.D. Miller, L.M. Pfeffer, J. Cancer Sci. Ther. 6 (2014) 370–377.
[74] B.B. Bagulkar, M. Gawande, M. Chaudhary, A.R. Gadbail, S. Patil, S. Bagulkar, XIAP and Ki-67: a correlation between antiapoptotic and proliferative marker expression in benign and malignant tumours of salivary gland: an immunohistochemical study, J. Clin. Diagn Res. 9 (2015), EC01-EC04, http://dx.doi.org/10.7860/JCDR/2015/11690.5604.
[75] X.P. Yi, T. Han, Y.X. Li, X.Y. Long, W.Z. Li, Simultaneous silencing of XIAP and survivin causes partial mesenchymal-epithelial transition of human pancreatic cancer cells via the PTEN/PI3K/Akt pathway, Mol. Med. Rep. 12 (2015) 601–608, http://dx.doi.org/10.3892/mmr.2015.3380.
[76] F. Lin, G. Ghislat, S. Luo, M. Renna, F. Siddiqi, D.C. Rubinsztein, XIAP and cIAP1 amplifications induce beclin 1-dependent autophagy through NFkB activation, Hum. Mol. Genet. 24 (2015) 2899–2913, http://dx.doi.org/10.1093/hmg/ddv052.
[77] M. Sanzey, S.A.A. Rahim, A. Oudin, A. Dirkse, T. Kaoma, L. Vallar, C. Herold-Mende, R. Bjerkvig, A. Golebiewska, S.P. Niclou, Comprehensive analysis of glycolytic enzymes as therapeutic targets in the treatment of glioblastoma, PLoS One 10 (2015), e0123544http://dx.doi.org/10.1371/journal.pone.0123544.
[78] D.L. Nelson, M.M. Cox, Chapter 12, Biological Membranes and Transport in Lehninger Principles of Biochemistry, 3rd ed. Worth Publishers, New York, NY, 2000 413.
[79] J.R. Casey, Why bicarbonate? Biochem. Cell Biol. 84 (2006) 930–939.
[80] J.W. Vince, R.A.F. Reithmeier, Carbonic anhydrase II binds to the carboxyl terminus of human band 3, the erythrocyte Cl−/HCO3- exchanger, J. Biol. Chem. 273 (1998) 28430–28437.
[81] P. Swietach, R.D. Vaughan-Jones, A.L. Harris, A. Hulikova, The chemistry, physiology and pathology of pH in cancer, Philos. Trans. R. Soc. Lond. Ser. B Biol. Sci. 369 (2014) 20130099, http://dx.doi.org/10.1098/rstb.2013.0099.